MARS CLIMATE DATABASE VERSION 4.3
VALIDATION DOCUMENT
- DRAFT -

E. Millour, F. Forget
(LMD, Paris)

May 2008

1. Introduction

This document presents comparisons between available data and outputs of the Mars Climate Database version 4.3.

The datasets of measurements which have been used in the comparisons detailed in this document are:

- *Surface temperature*, *atmospheric temperature* and *water vapour column* retrieved by the Thermal Emission Spectrometer (TES) onboard Mars Global Surveyor. TES has monitored the Martian atmosphere nearly continuously for almost three full Martian years from mid-Martian year 24[1] ("MY24") until early MY27. MGS being in a near-polar, sun-synchronous orbit, data was obtained for Local Solar times of 2 and 14 Martian hours (i.e. nighttime and daytime). The primary mode of TES data acquisition is nadir viewing. The up-to-date data used in this document was provided by M.D. Smith (NASA Goddard Space Flight Center) in april 2007. Note that the the TES data are binned in bins that are 5 degrees in Ls, 3 degrees in latitude, and 7.5 degrees in longitude. As a results, a major part of the day-to-day variability due to atmospheric waves is smoothed out. This makes them suitable for comparison with the MCD predictions without "perturbation" added.
- *Atmospheric temperature* derived from radio occultation using the ultrastable oscillator onboard MGS, starting in Mars Year 24 and well into Mars Year 27. Data were provided by Dave Hinson, Stanford University.
- *Surface pressure* recorded by the Viking landers and Pathfinder.

[1] The Martian years are numbered according to the now widely used calendar proposed by R. Todd Clancy (Clancy et al., *Journal of Geophys. Res* 105, p 9553, 2000) which starts on april 11, 1955 (Mars Northern Spring Equinox, Ls=0^{o}). Martian 24, 25, 26 ended respectively around 03/07/2000, 26/05/2002, 07/05/2004.

2. Comparison with TES surface temperature

TES records extend from mid-MY24 (Ls=102.5) until early MY27 (Ls=85). The baseline dust scenario “MY24 scenario” in the MCD is based on assimilation of TES dust over MY24-MY25; the first set of comparisons is thus focused on this period (i.e. over slightly more than a Martian year, starting at Ls=102.5 in MY24 until Ls=180 in MY25; slightly before the global dust storm that occurred then).
Data collected from the beginning of MY26 until Ls=85 in MY27 is then compared to the MCD outputs of the baseline “MY24” scenario in order to check and assess its genericity.

2.1 Comparisons over MY24-MY25

Daytime (2pm, local time) and nighttime (2am, local time) zonal surface temperature over MY24-MY25 measured by TES and obtained using the MCD are given in figures 2.1 and 2.3. The differences between MCD and TES datasets are displayed in figures 2.2 and 2.4. note that the most drastic differences occur at high latitudes and correspond to a small temporal lag (between the MCD prediction and TES measurements) in the progression or retreat of the CO2 ice cap.
To exclude this bias, distributions of surface temperature differences between MCD v4.3 and TES that are given in figure 2.5 are computed for data in the [50°S-50°N] latitude band. As can be seen in the figure, the agreement between datasets is good: the mean difference between MCD predictions and TES measurements is less than 1K.
Maps of mean surface temperature differences between MCD and TES values, for daytime (2pm, local solar time) and nighttime (2am, local solar time) are given in figure 2.6.

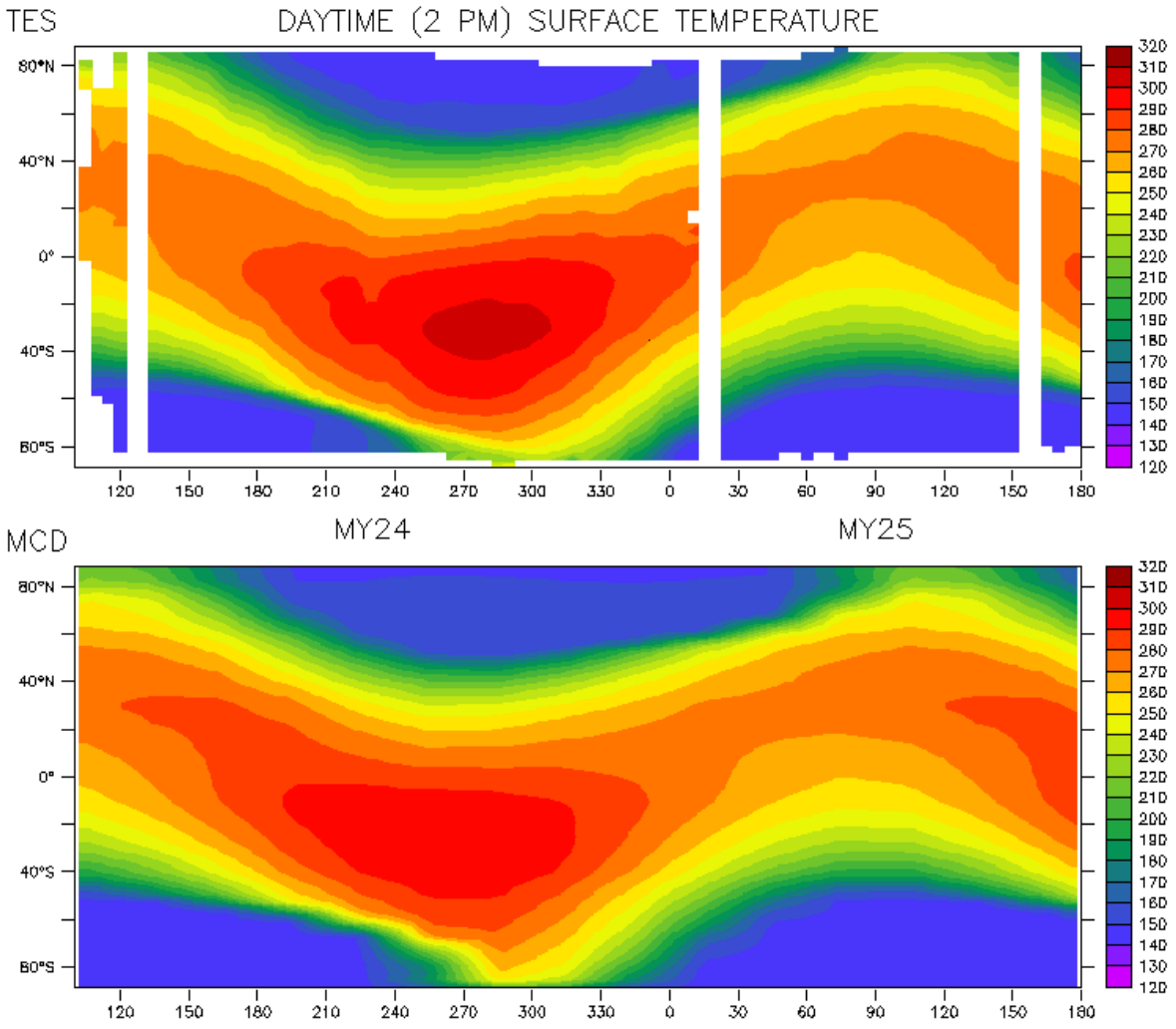

Figure 2.1 :Zonal surface temperature over Martian Years 24-25, at 2 pm (local solar time). Top: TES data. Bottom MCD data.

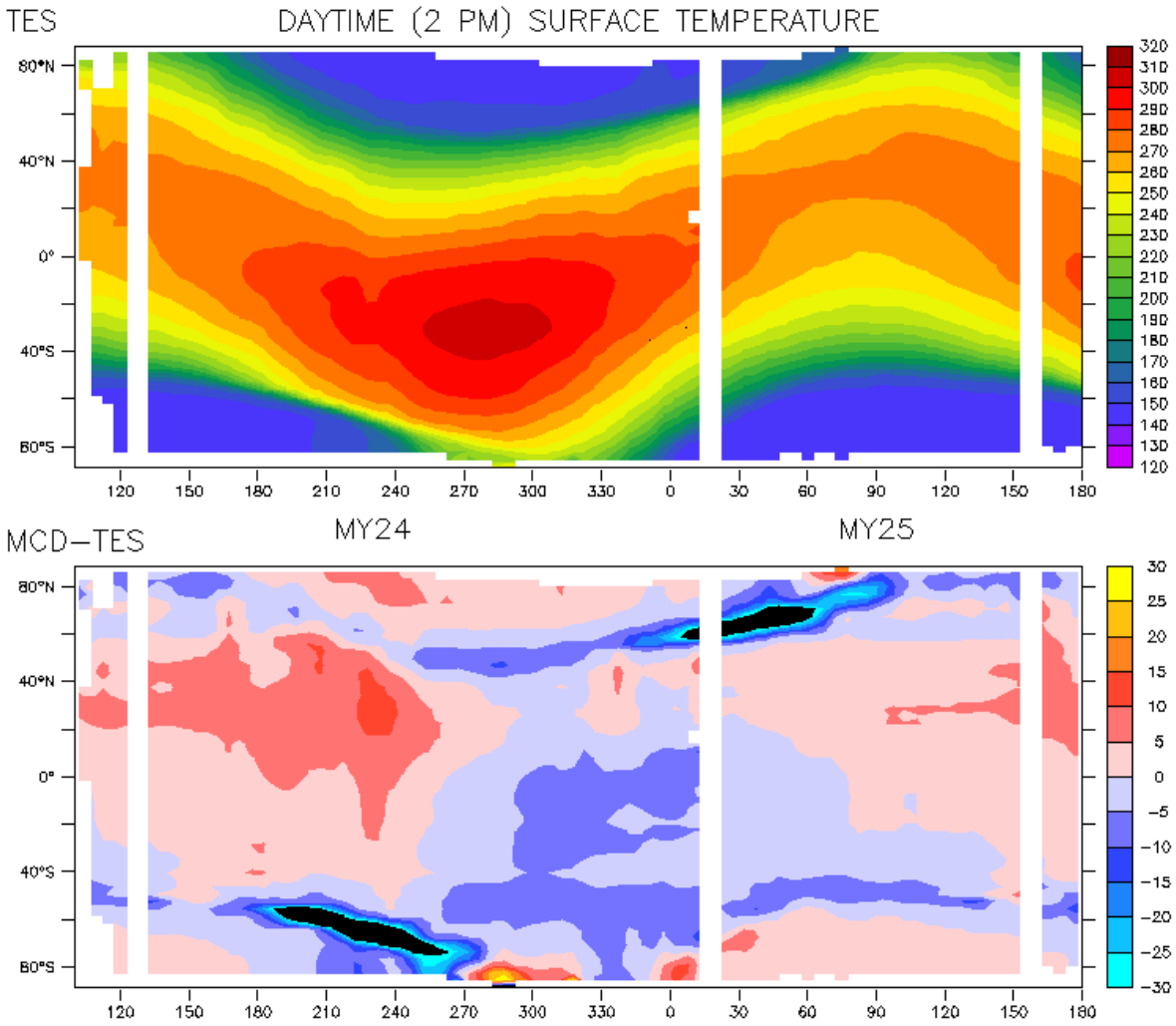

Figure 2.2 : Top : Zonal surface temperature over Martian Years 24-25, at 2 pm (local solar time) measured by TES. Bottom: Difference between MCD and TES data; black areas correspond to differences between -30 and -70 K which are due to temporal lags between the progression or retreat of CO2 ice.

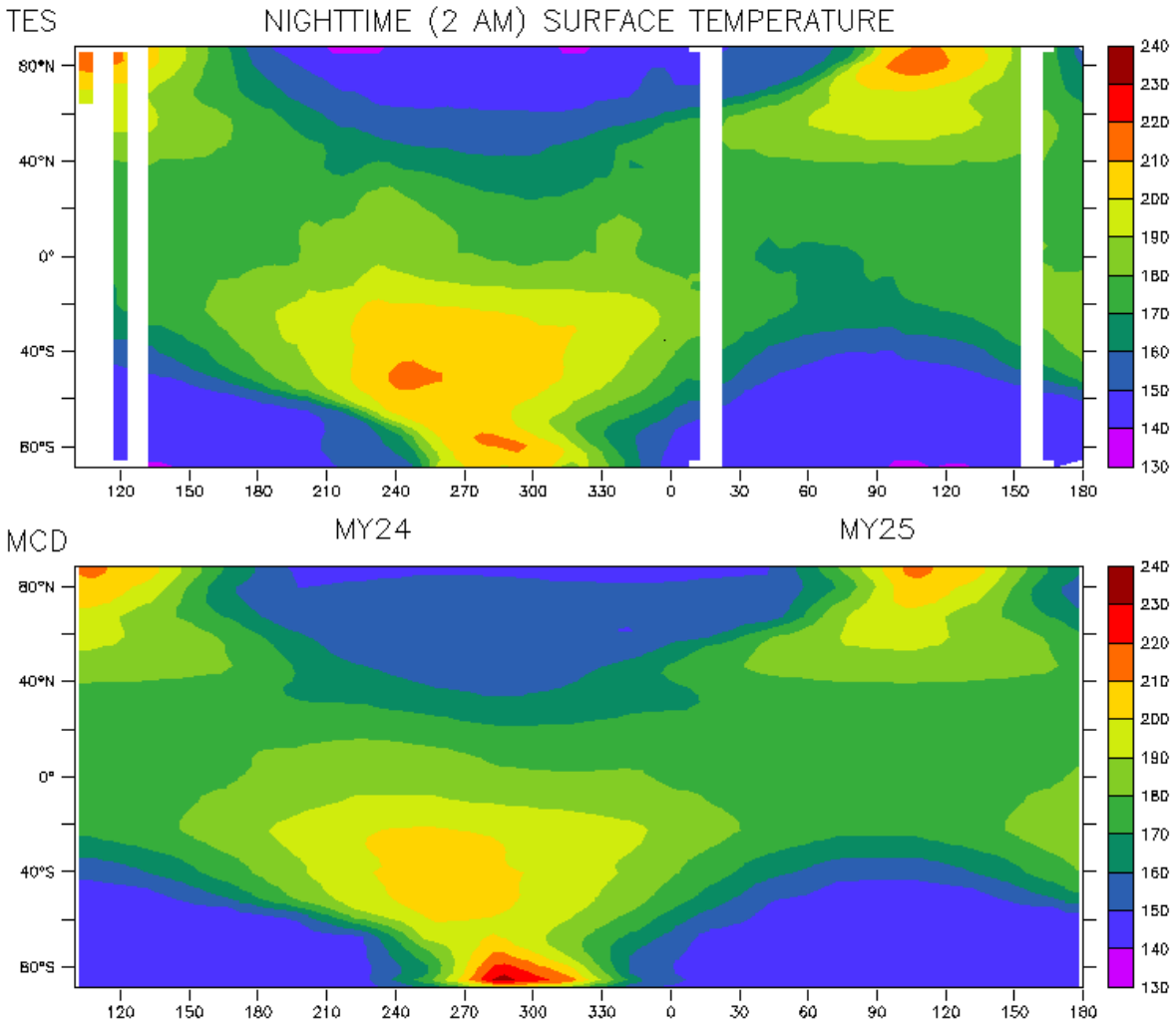

Figure 2.3 : Zonal surface temperature over Martian Years 24-25, at 2 am (local solar time). Top : TES data. Bottom : MCD data.

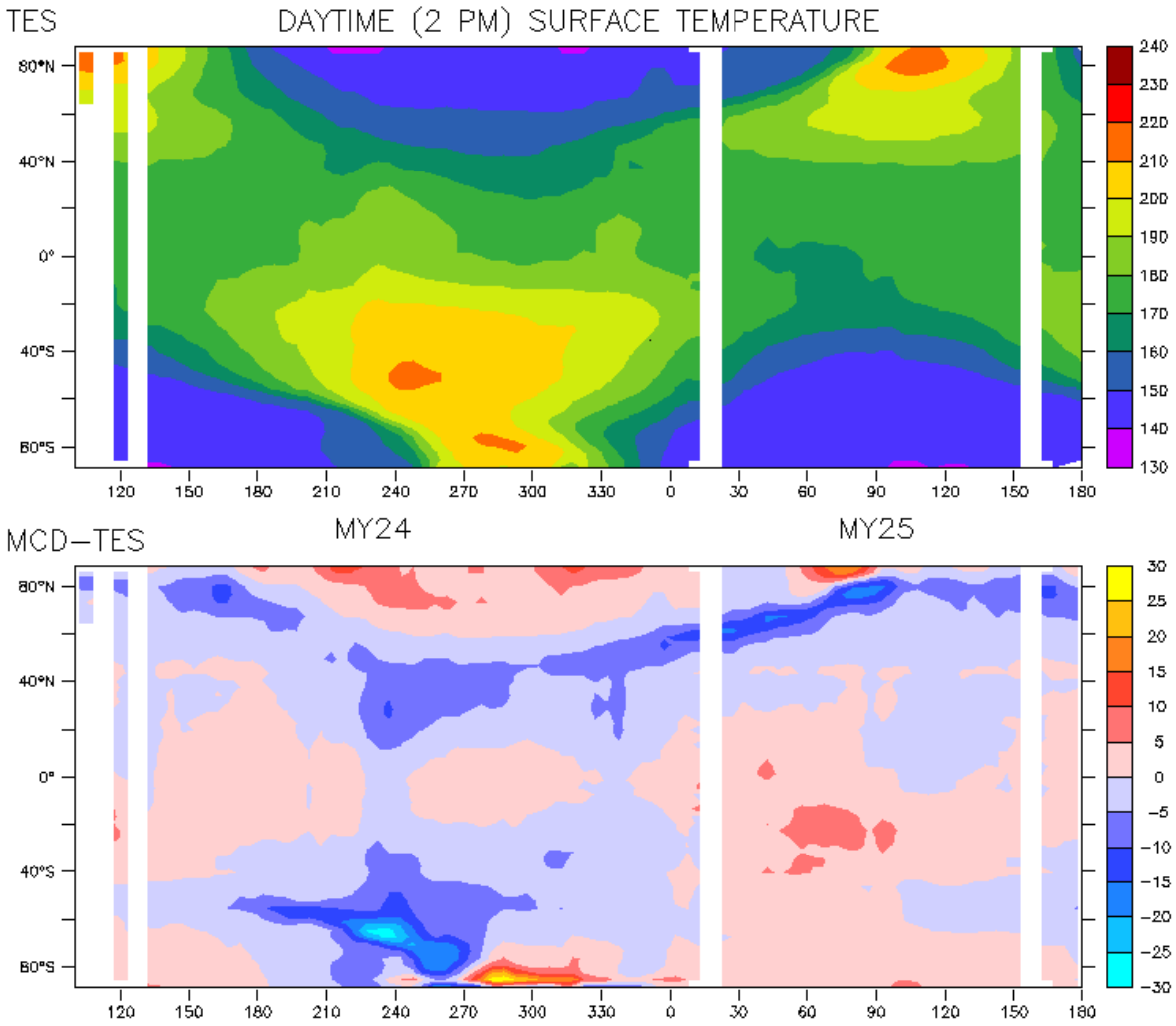

Figure 2.4 : Top : Zonal surface temperature over Martian Years 24-25, at 2 pm (local solar time) measured by TES. Bottom: Difference between MCD and TES data.

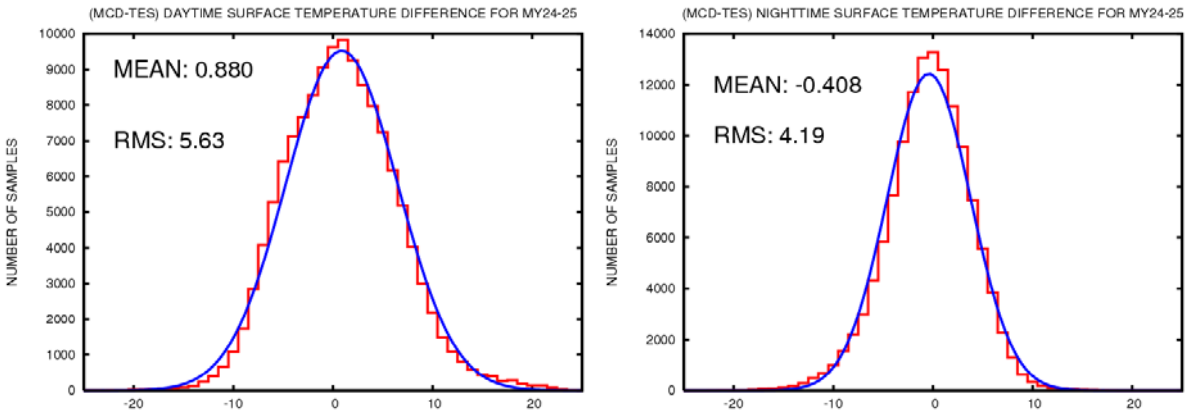

Figure 2.5 : Distribution of surface temperature differences between MCD v4.3 and TES. Statistics were computed over Mars Years 24 and 25 (from Ls=102.5 in MY24 until Ls=180 in MY25) and for data in the [50S : 50N] latitude band, using bins of 1K. Given mean and RMS values are computed for the histograms; the blue curves are normal distributions of same mean and RMS. Left plot is for daytime data (i.e. at 2pm, local solar time) end right plot is for nighttime (i.e. 2am, local solar time) data.

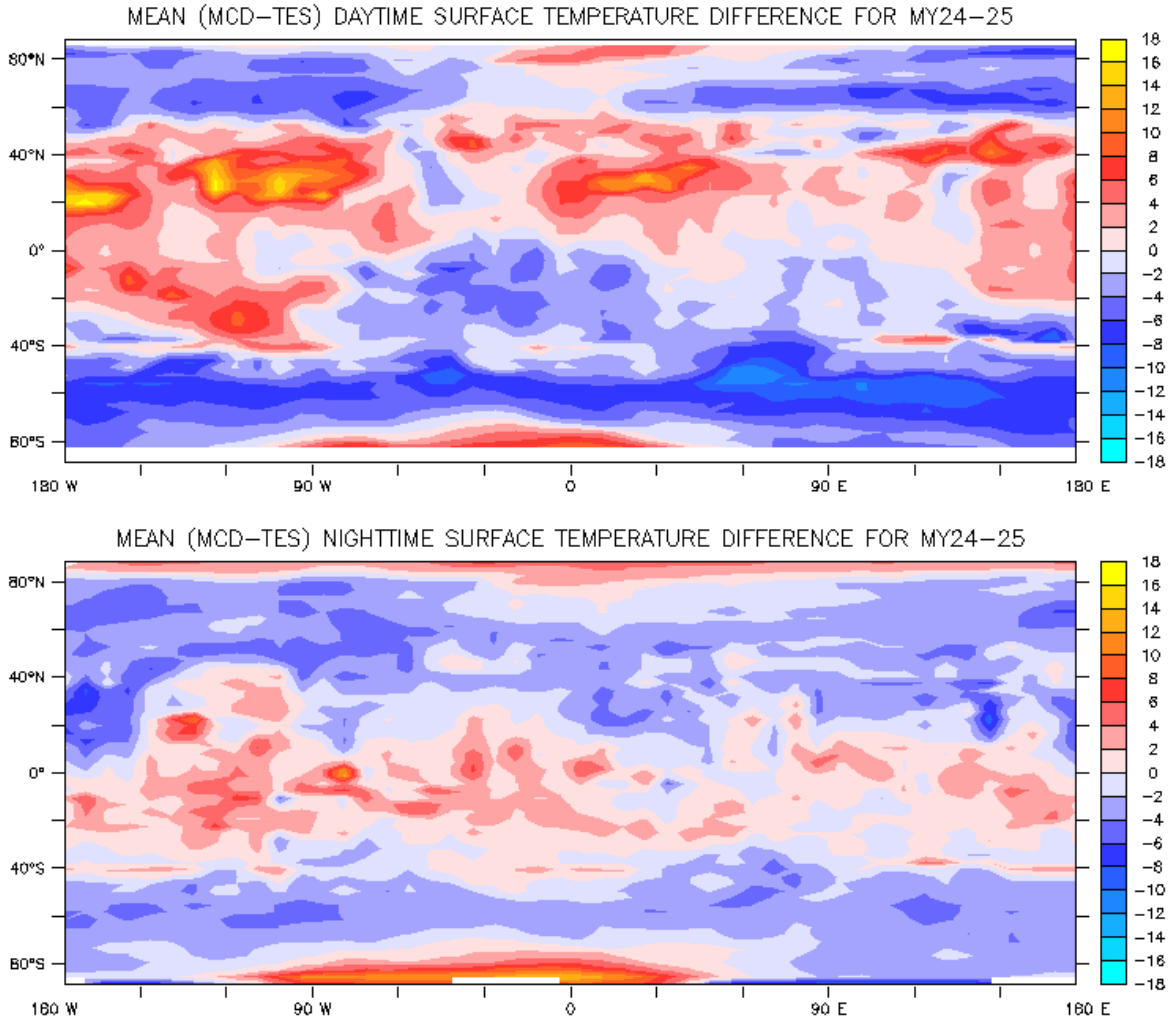

Figure 2.6 : Longitude-latitude maps of the mean (taken over time period starting at Ls=102.5 in MY24 and ending at LS=180 in MY25) difference between TES and MCD surface temperature. Top: Daytime (2am, local solar time) difference. Bottom: Nighttime (2pm, local solar time) difference.

2.2 Comparisons over MY26-MY27

In order to check the generality of the MCD baseline “MY24” scenario, the same kind of surface temperature comparisons that were presented in section 2.1, but this time with TES data obtained during Mars Years 26 (and the beginning of Mars Year 27, up to Ls=85) are presented here.

Figures 2.7 and 2.9 display TES and MCD surface temperatures and their differences are shown in figures 2.8 and 2.10. Note that there was in Mars Year 26 (around Ls=320-330) severe local storm which did not occur in Mars Year 24 and thus yields greater differences between MCD and TES data at that time. Despite this, the distributions of TES and MCD surface temperature differences (again evaluated in the [50°S-50°N] latitude band) given in figure 2.11 shows the good agreement between datasets.
Maps of mean surface temperature differences between MCD and TES values, for daytime (2pm, local solar time) and nighttime (2am, local solar time) are given in figure 2.6.

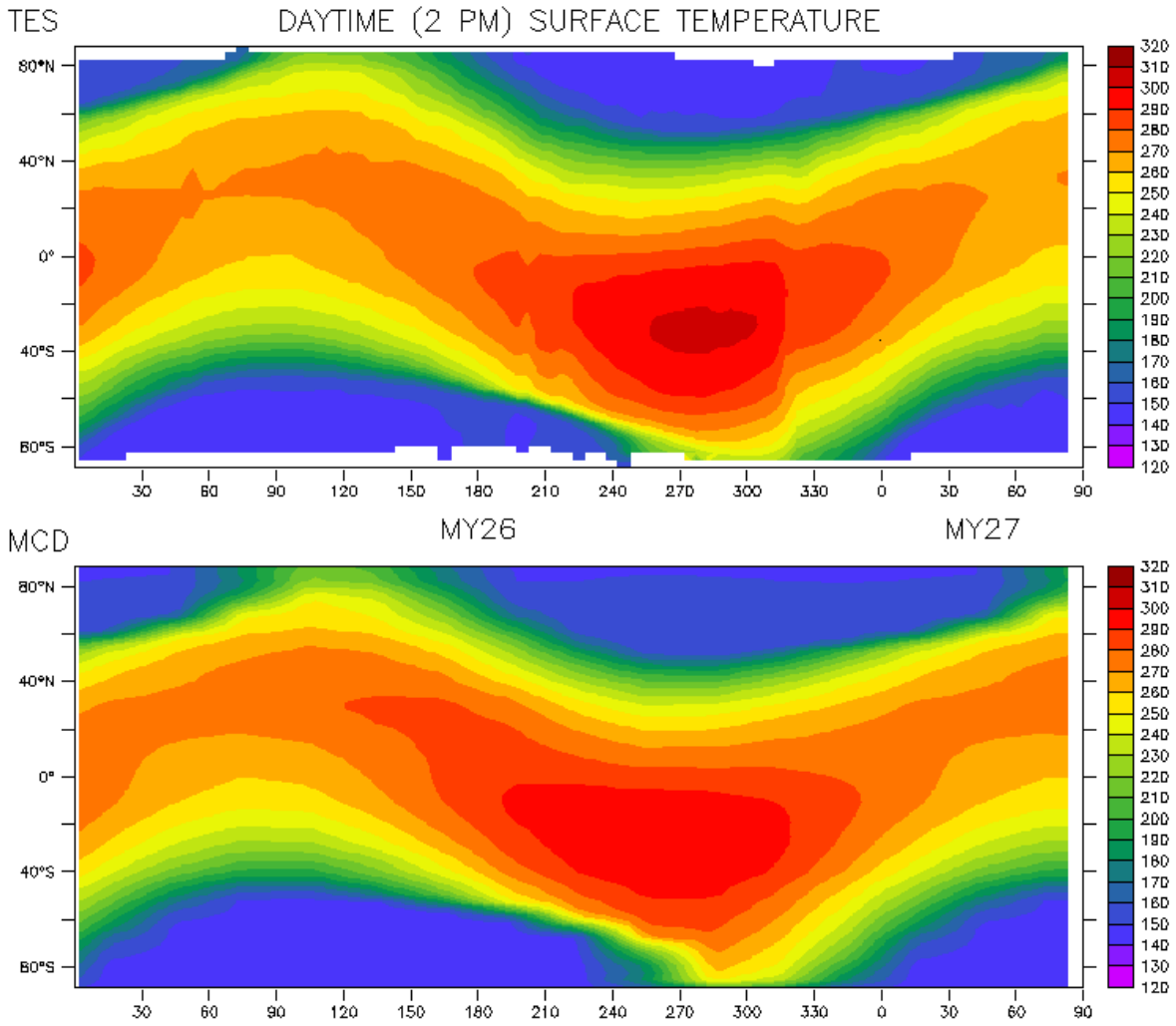

Figure 2.7 :Zonal surface temperature over Martian Years 26-27, at 2 pm (local solar time). Top: TES data. Bottom: MCD data.

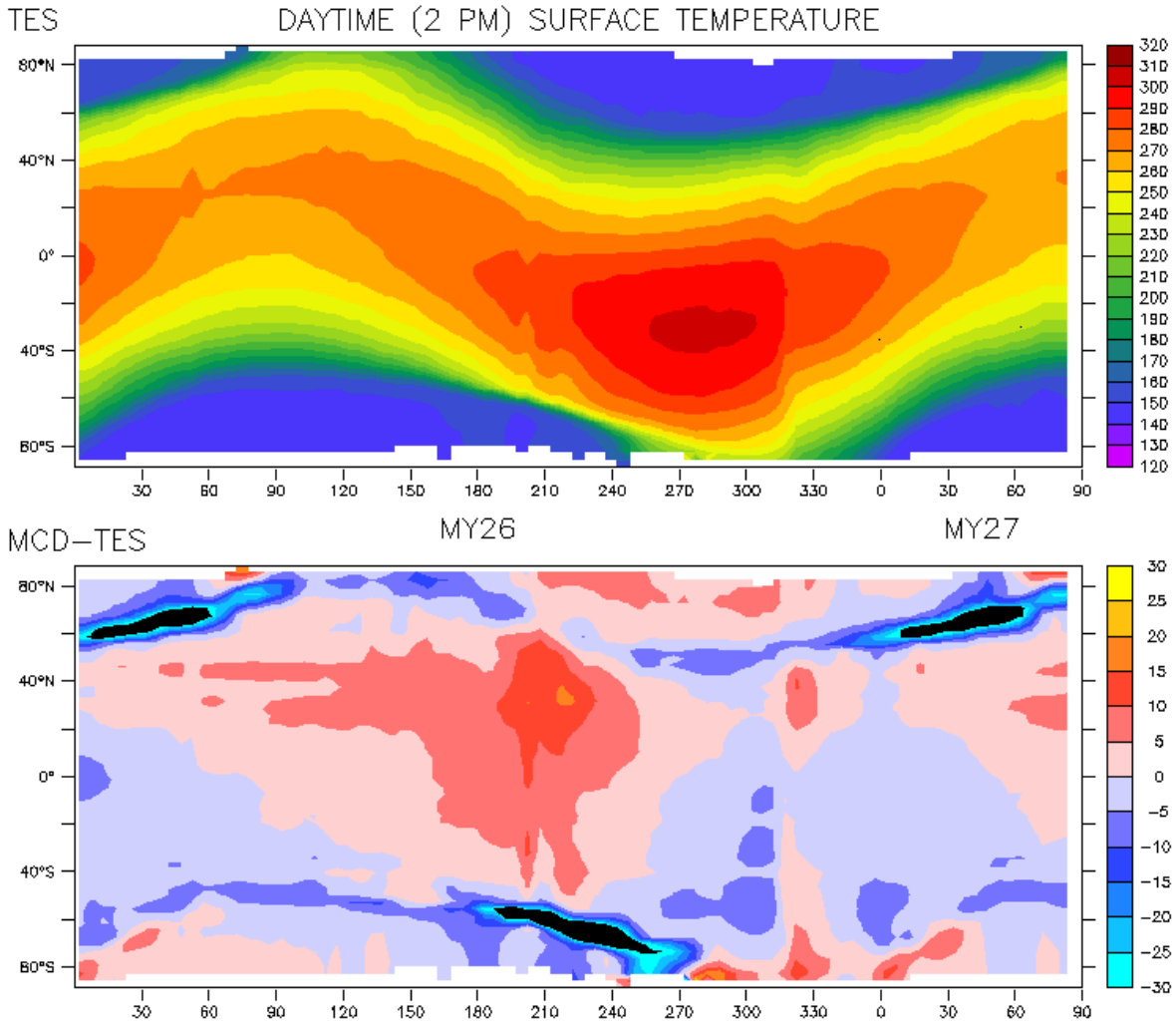

Figure 2.8 : Top : Zonal surface temperature over Martian Years 26-27, at 2 pm (local solar time) measured by TES. Bottom: Difference between MCD and TES data; black areas correspond to differences between -30 and -70 K which are due to lags between the progression or retreat of CO2 ice.

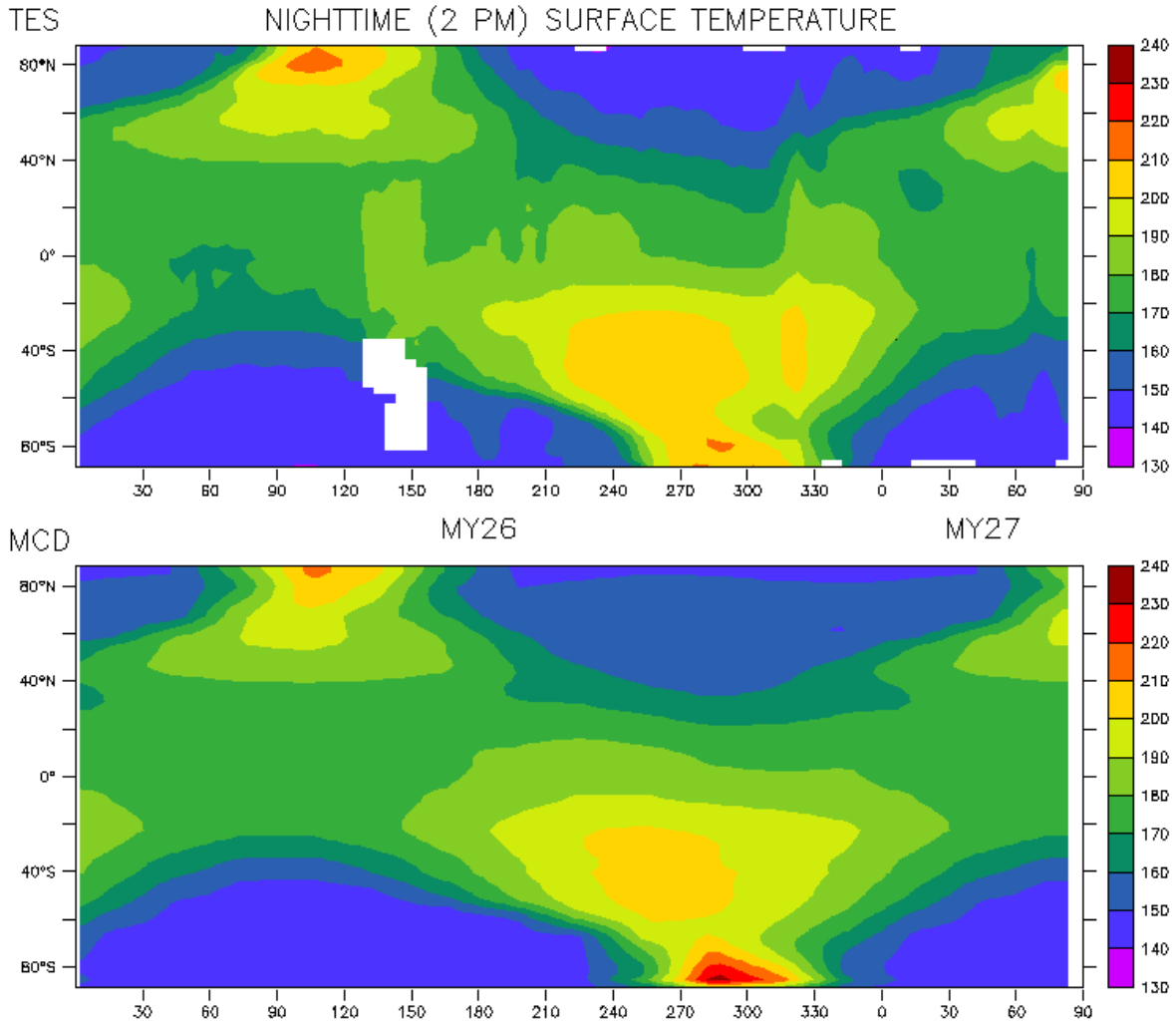

Figure 2.9 : Zonal surface temperature over Martian Years 26-27, at 2 am (local solar time). Top: TES data. Bottom: MCD data.

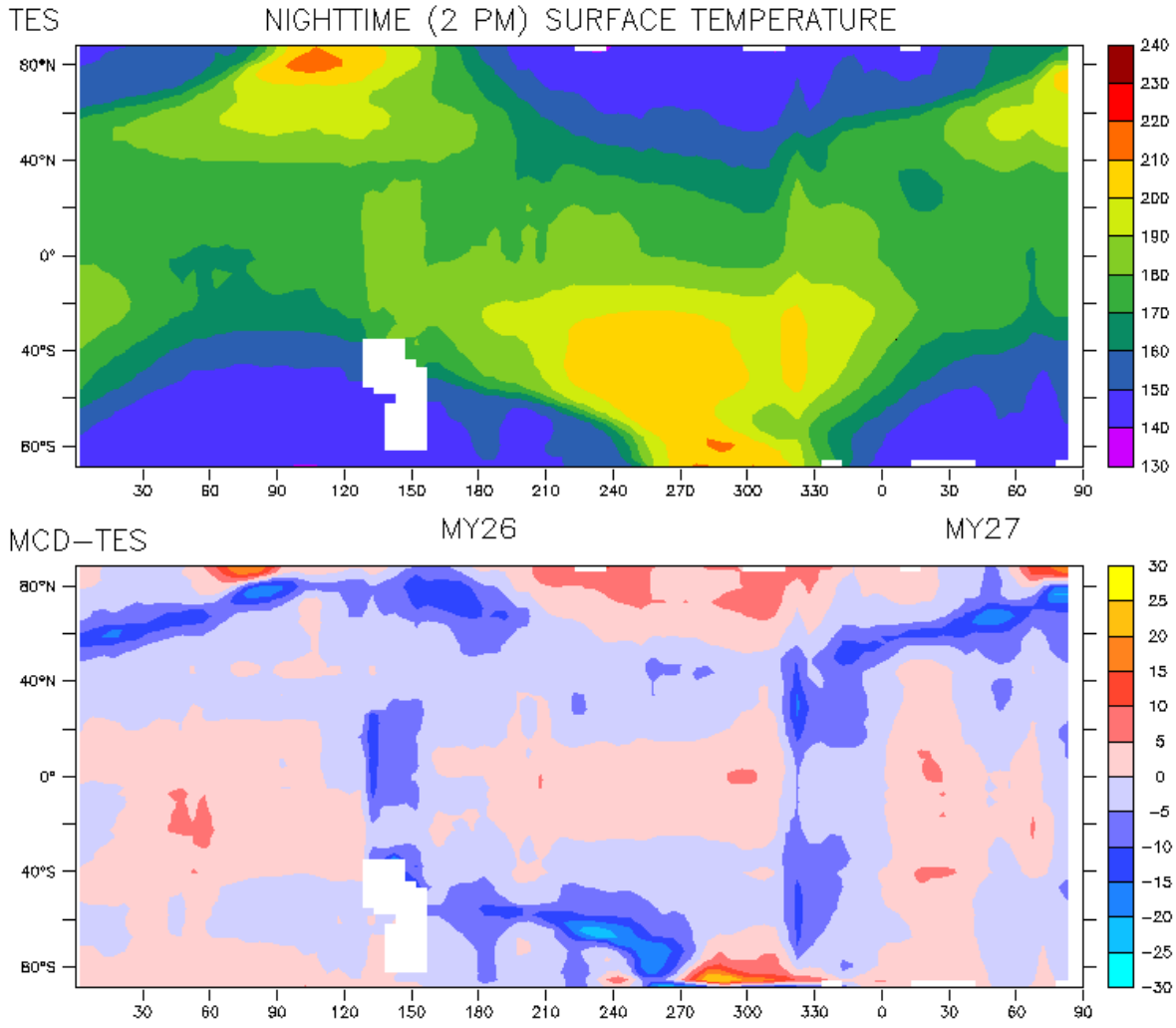

Figure 2.10 : Top : Zonal surface temperature over Martian Years 26-27, at 2 am (local solar time) measured by TES. Bottom: Difference between MCD and TES data.

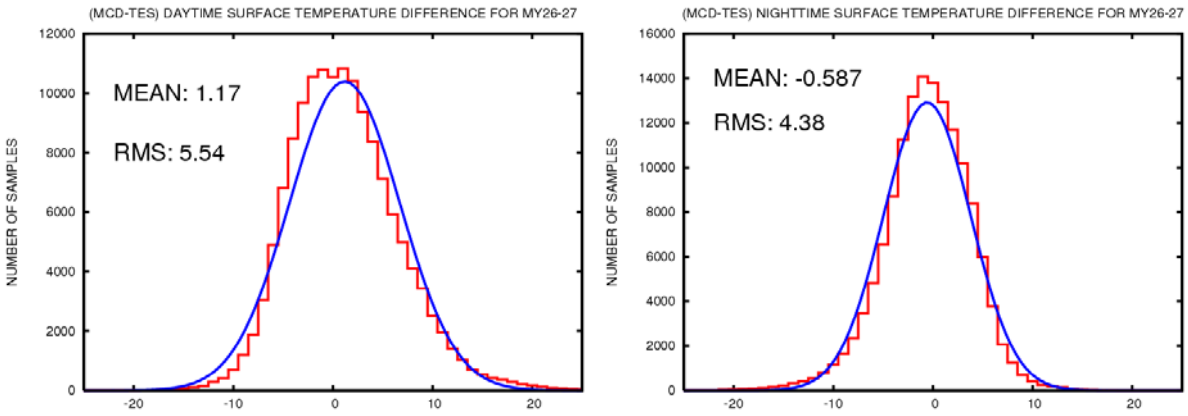

Figure 2.11 : Distribution of surface temperature differences between MCD v4.3 and TES. Statistics were computed over Mars Years 26 and 27 (from Ls=0 in MY26 until Ls=85 in MY27) and for data in the [50S : 50N] latitude band, using bins of 1K. Given mean and RMS values are computed for the histograms; the blue curves are normal distributions of same mean and RMS. Left plot is for daytime data (i.e. at 2pm, local solar time) end right plot is for nighttime (i.e. 2am, local solar time) data.

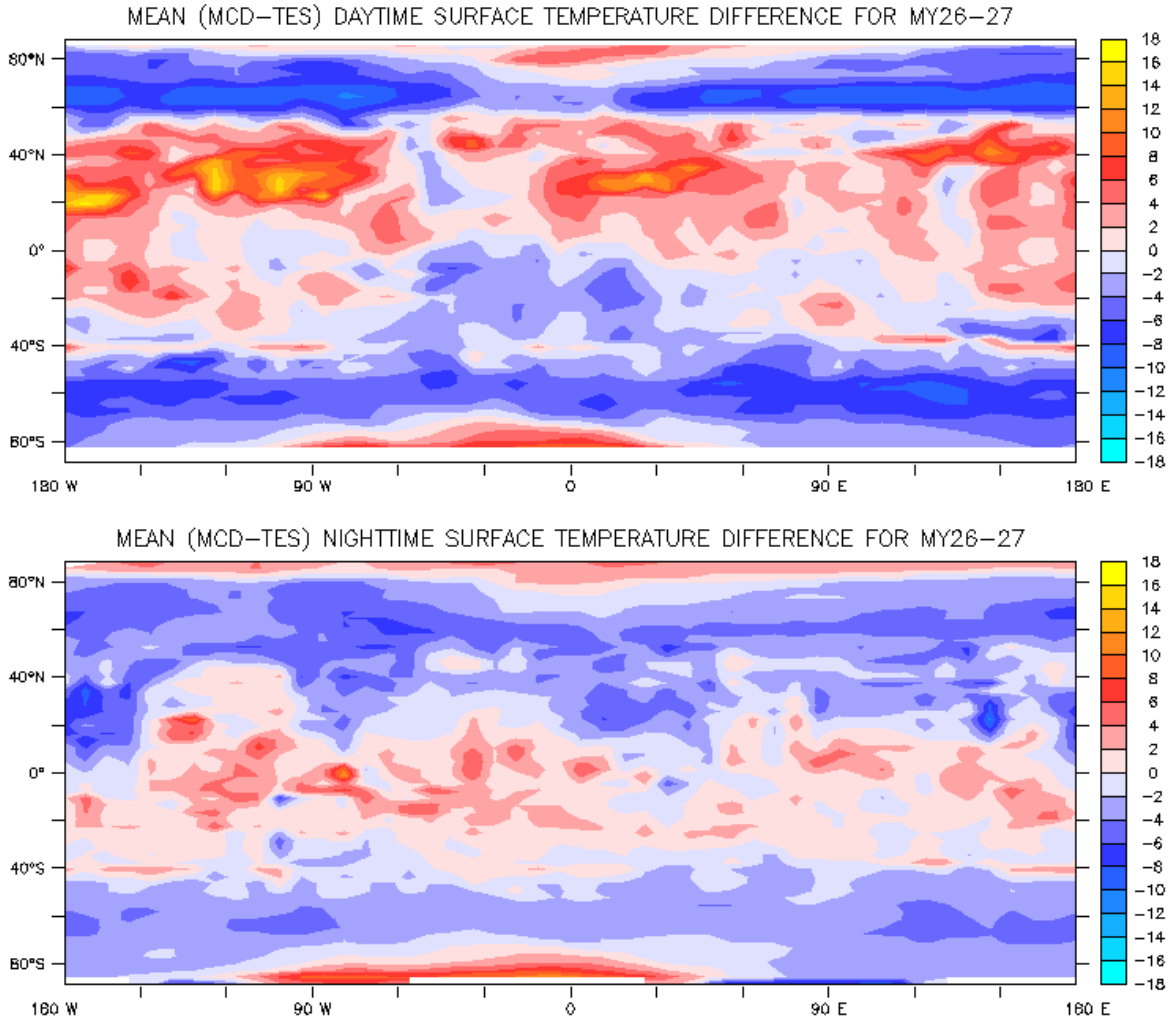

Figure 2.12 : Longitude-latitude maps of the mean (taken over time period starting at Ls=0 in MY26 and ending at Ls=85 in MY27) difference between TES and MCD surface temperature. Top: Daytime (2am, local solar time) difference. Bottom: Nighttime (2pm, local solar time) difference.

3. Comparison with Radio Occultation atmospheric temperature

Thermal profiles have been retrieved by radio occultation, measurements which use an ultrastable oscillator onboard MGS and monitor its signal during occultation entries and exits between MGS, Mars and tracking stations on Earth.

The distribution of available radio occultation thermal profiles in latitude, solar longitude and local time are given in figure 3.1.

Note that when comparing this dataset with the MCD (using the baseline “MY24” scenario), only the [50°S-50°N] latitudinal band was considered, and that comparisons excluded data obtained during the MY25 global dust storm. Only nighttime data was thus available for comparison.

Distributions of atmospheric temperature differences between MCD prediction and radio-occultation profiles are displayed in figure 3.2 and 3.3, when only Mars Year 24 data is considered, for four heights intervals of 10 km.

Figures 3.4 and 3.5 similarly display the distributions of atmospheric temperature differences between MCD prediction and radio-occultation profiles when all data (except at high latitudes or during the MY25 global dust storm) is considered.

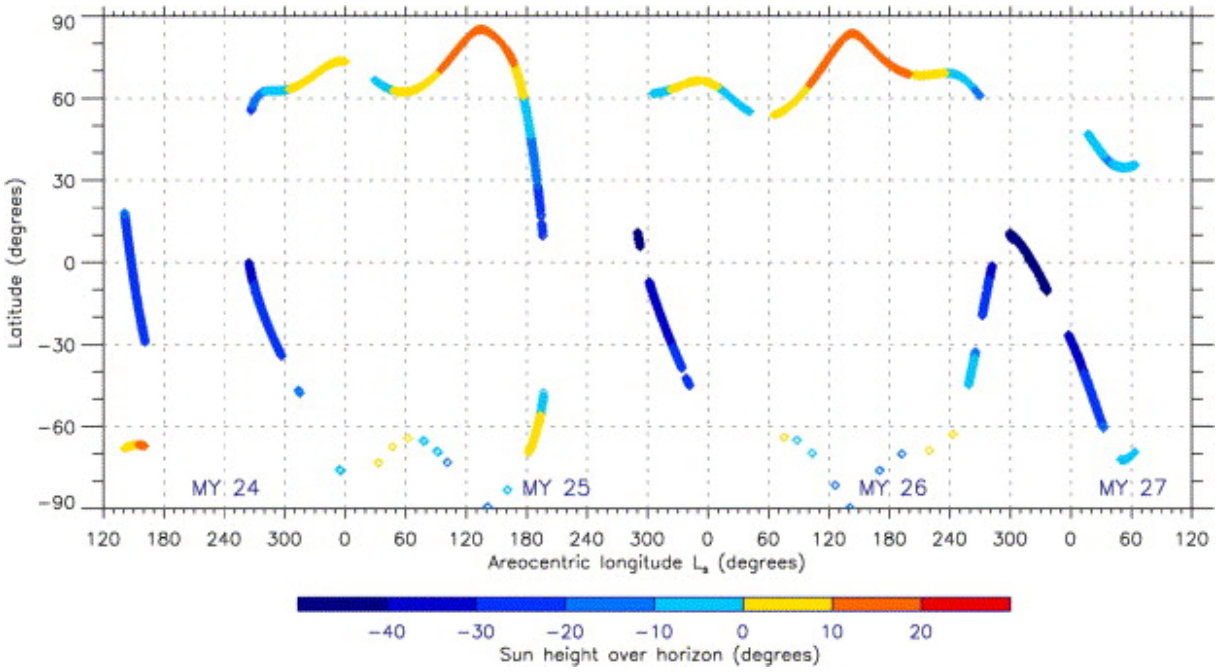

Figure 3.1 : Figure from Montabone et al., Icarus 185 (2006) 113-132. Distribution of available radio occultation thermal profiles in latitude, aerocentric longitude and solar altitude (height of the Sun over the horizon). Colours refer to different solar altitudes in degrees (blueish colours for night profiles, yellowish colours for daylight profiles).

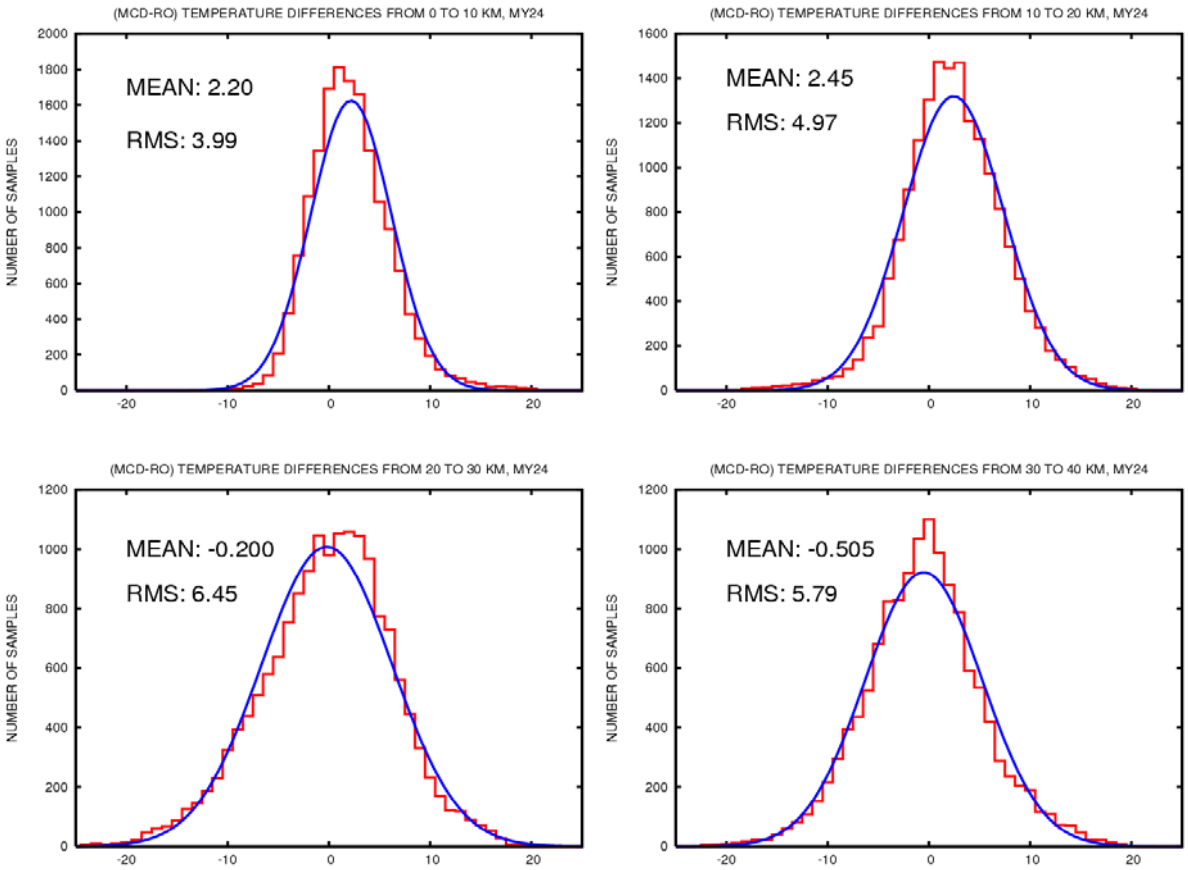

Figure 3.2 : Distributions of atmospheric temperature differences between MCD and Radio Occultation profiles. Statistics computed for Mars Year 24 data within the 50S-50N latitude band, using bins of 1K, along altitude bands of 10 km. Given mean and RMS values are computed for the histograms; the blue curves are normal distributions of same mean and RMS.

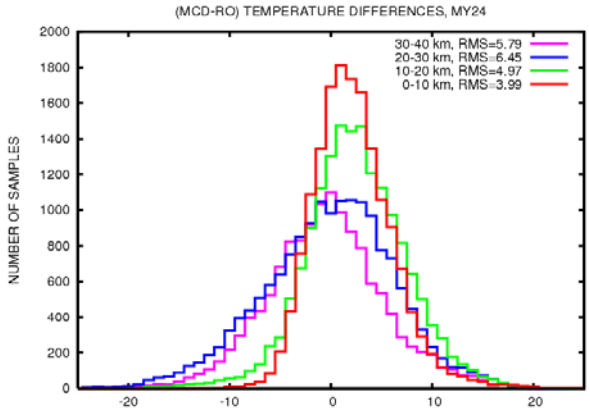

Figure 3.3 : Same distributions of atmospheric temperature differences as given in figure 3.1, plotted at once to display the evolution of RMS with altitude.

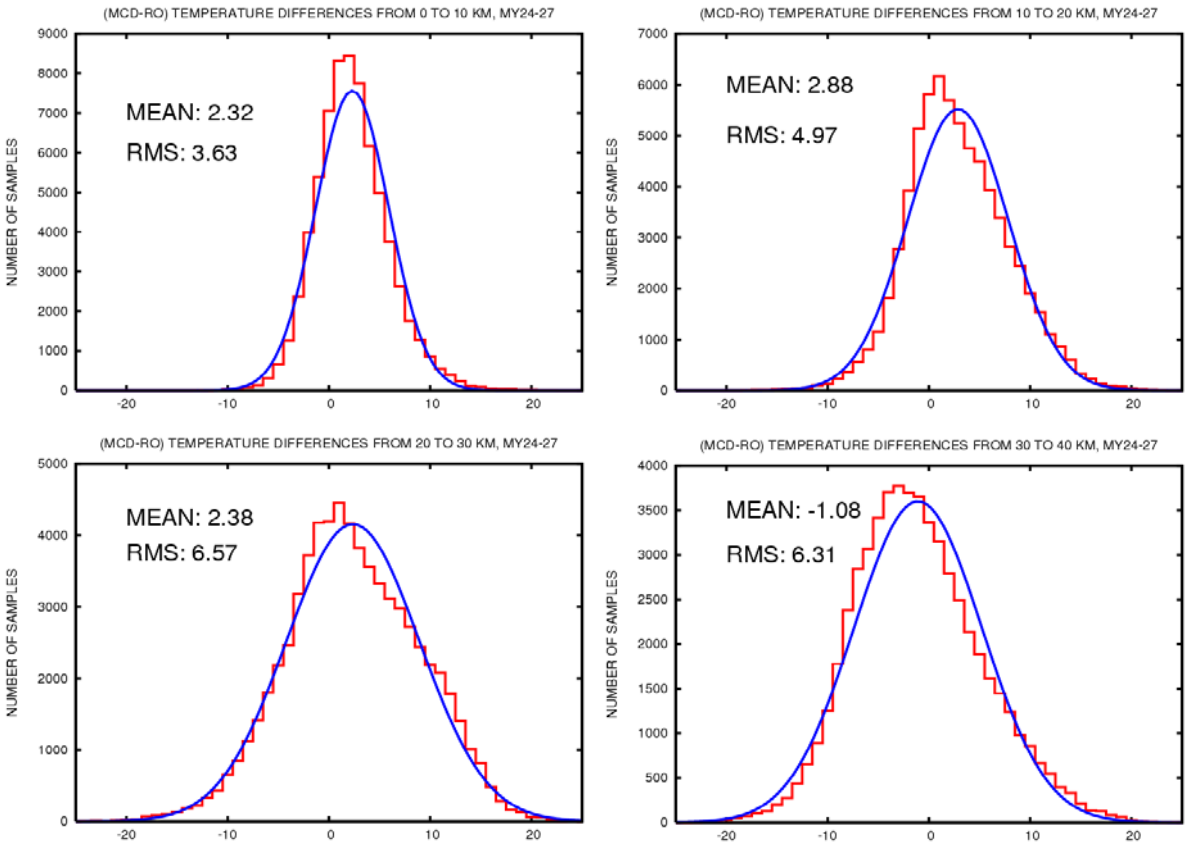

Figure 3.4 : Distributions of atmospheric temperature differences between MCD and Radio Occultation profiles. Statistics computed for Mars Year 24-27 data (except during MY25 global dust storm) within the 50S-50N latitude band, using bins of 1K, along altitude bands of 10 km. Given mean and RMS values are computed for the histograms; the blue curves are normal distributions of same mean and RMS.

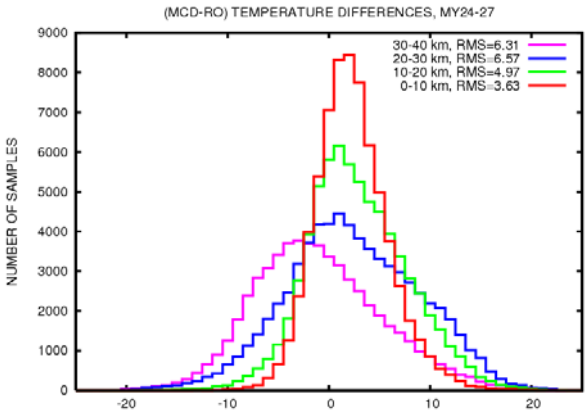

Figure 3.5 : Same distributions of atmospheric temperature differences as given in figure 15, plotted at once to display the evolution of RMS with altitude.

4. Comparison with TES atmospheric temperature

TES datasets include atmospheric temperature, which we here compare to MCD predictions. Comparisons were made at two given pressure levels

- 106 Pa, around 15-20 km altitude where TES Nadir retrieval is most accurate (peak of the weighting function)
- 5.28 Pa, around 40-45 km altitude where TES limb retrieval is the most reliable.

4.1 Comparisons with MY24-MY25 data

As for the surface temperature comparison, two separate sets of comparisons are made: one for MY24-MY25, and the other for MY26-MY27.

4.1.1 Atmospheric temperature at 106 Pa and 5.28 Pa

As for the surface temperature comparisons, figures 4.1 to 4.12 display daytime and nighttime temperature differences between MCD predictions and TES measurements.

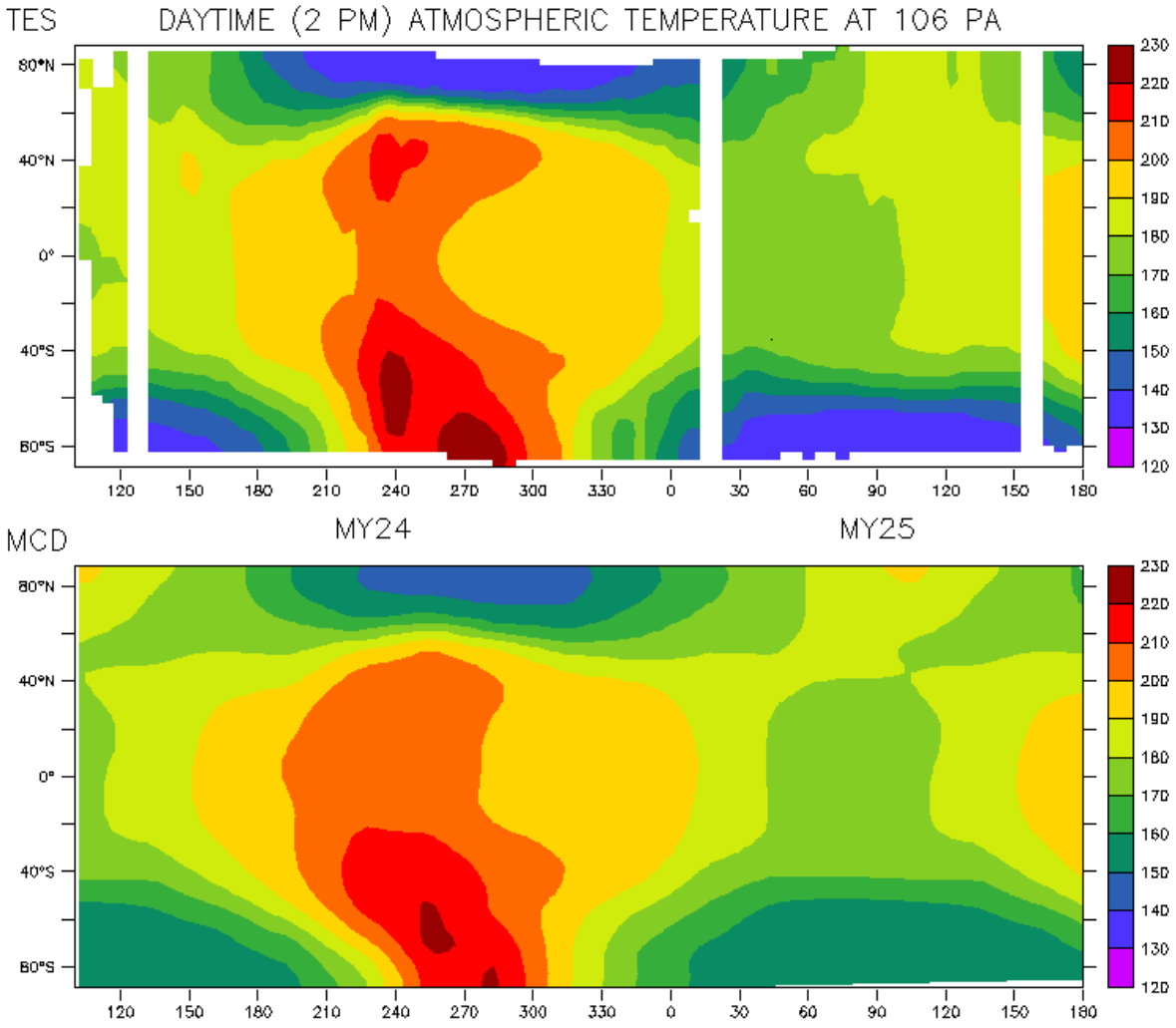

Figure 4.1 : Zonal values of atmospheric temperature at 106 Pa over Mars Years 24 and 25, at 2pm (local solar time). Top: TES measurements. Bottom: MCD.

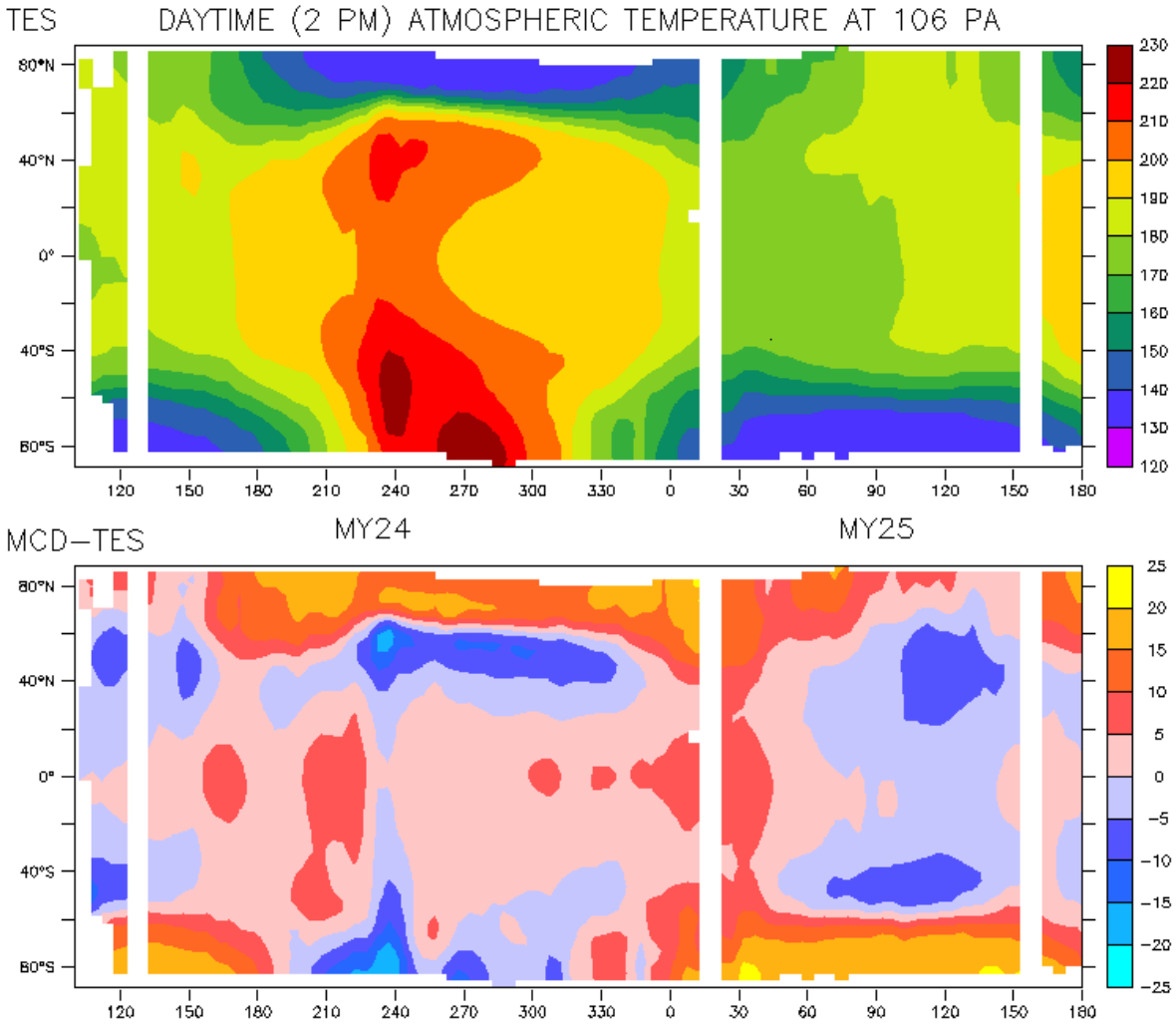

Figure 4.2 : Top : Zonal atmospheric temperature at 106 Pa, over Martian Years 24-25, at 2pm (local solar time) measured by TES. Bottom: Difference between MCD and TES data.

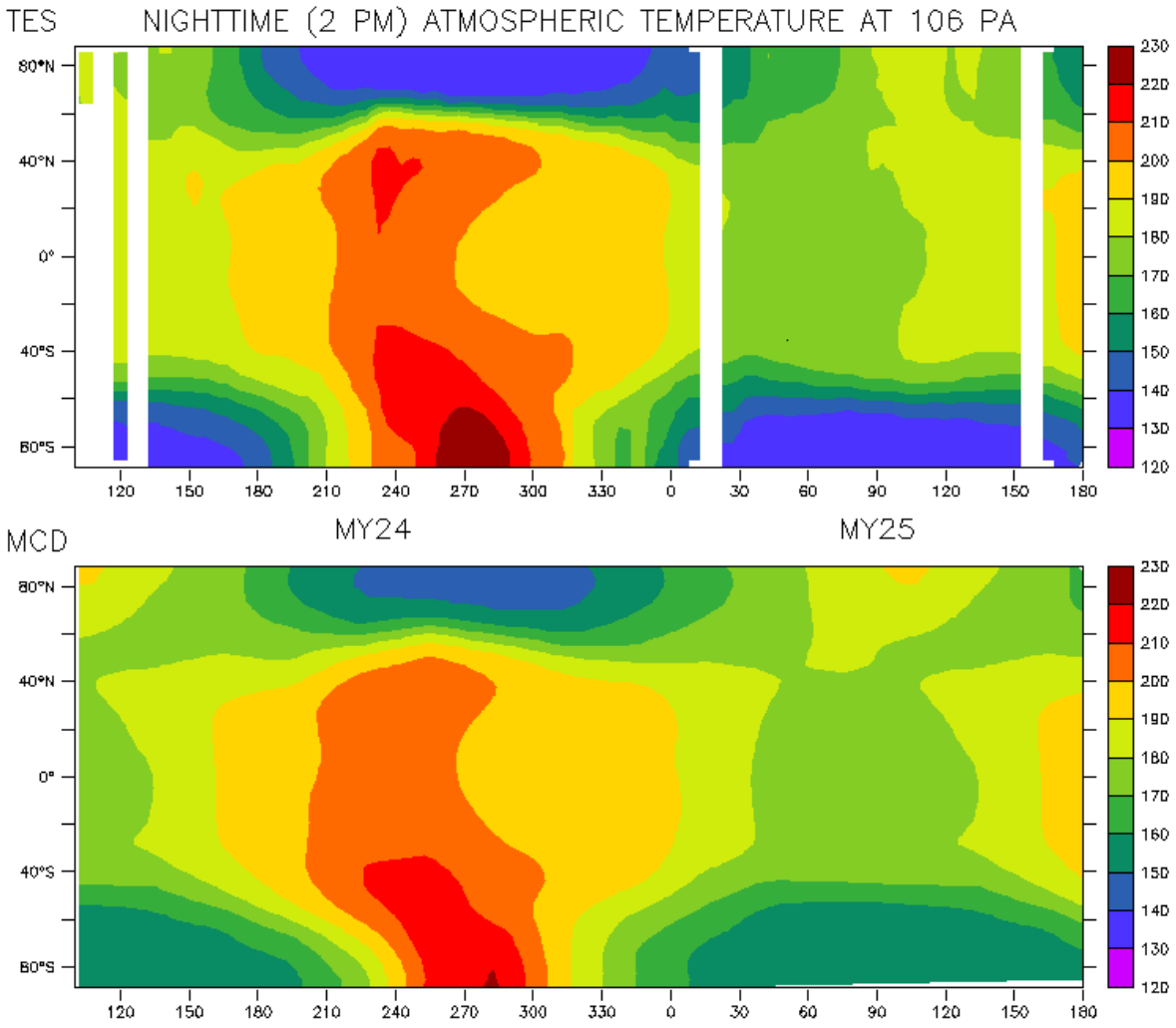

Figure 4.3 : Zonal values of atmospheric temperature at 106 Pa over Mars Years 24 and 25, at 2am (local solar time). Top: TES measurements. Bottom: MCD.

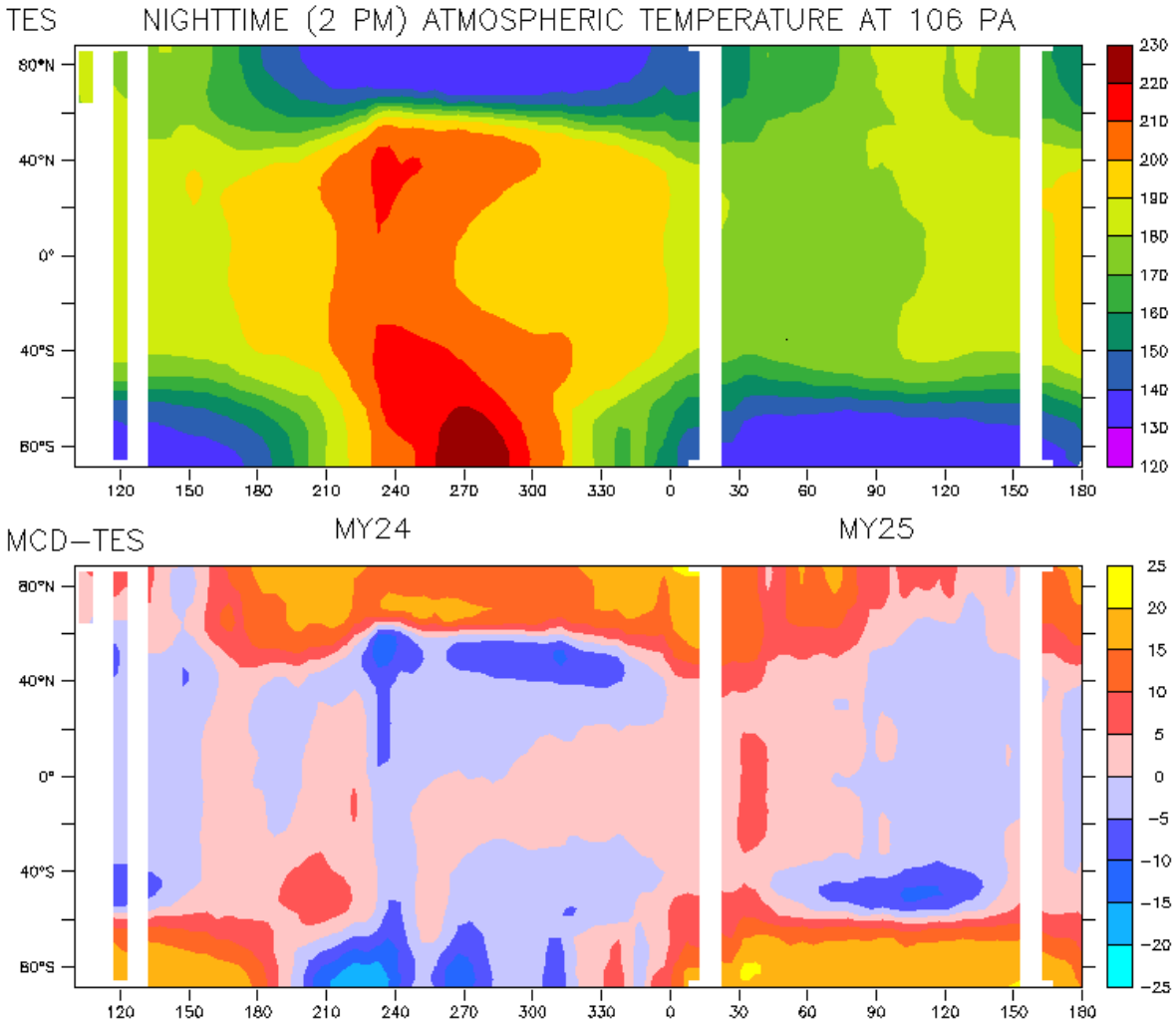

Figure 4.4 : Top : Zonal atmospheric temperature at 106 Pa, over Martian Years 24-25, at 2am (local solar time) measured by TES. Bottom: Difference between MCD and TES data.

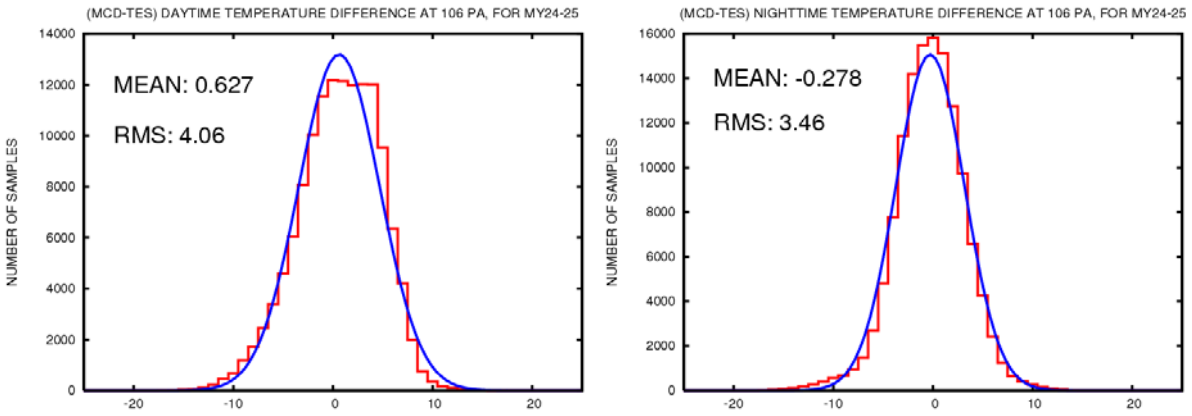

Figure 4.5 : Distribution of atmospheric temperature differences, at 106 Pa, between MCD and TES. Statistics were computed over Mars Years 24 and 25 (from Ls=102.5 in MY24 until Ls=180 in MY25) and for data in the [50S : 50N] latitude band, using bins of 1K. Given mean and RMS values are computed for the histograms; the blue curves are normal distributions of same mean and RMS. Left plot is for daytime data (i.e. at 2pm, local solar time) end right plot is for nighttime (i.e. 2am, local solar time) data.

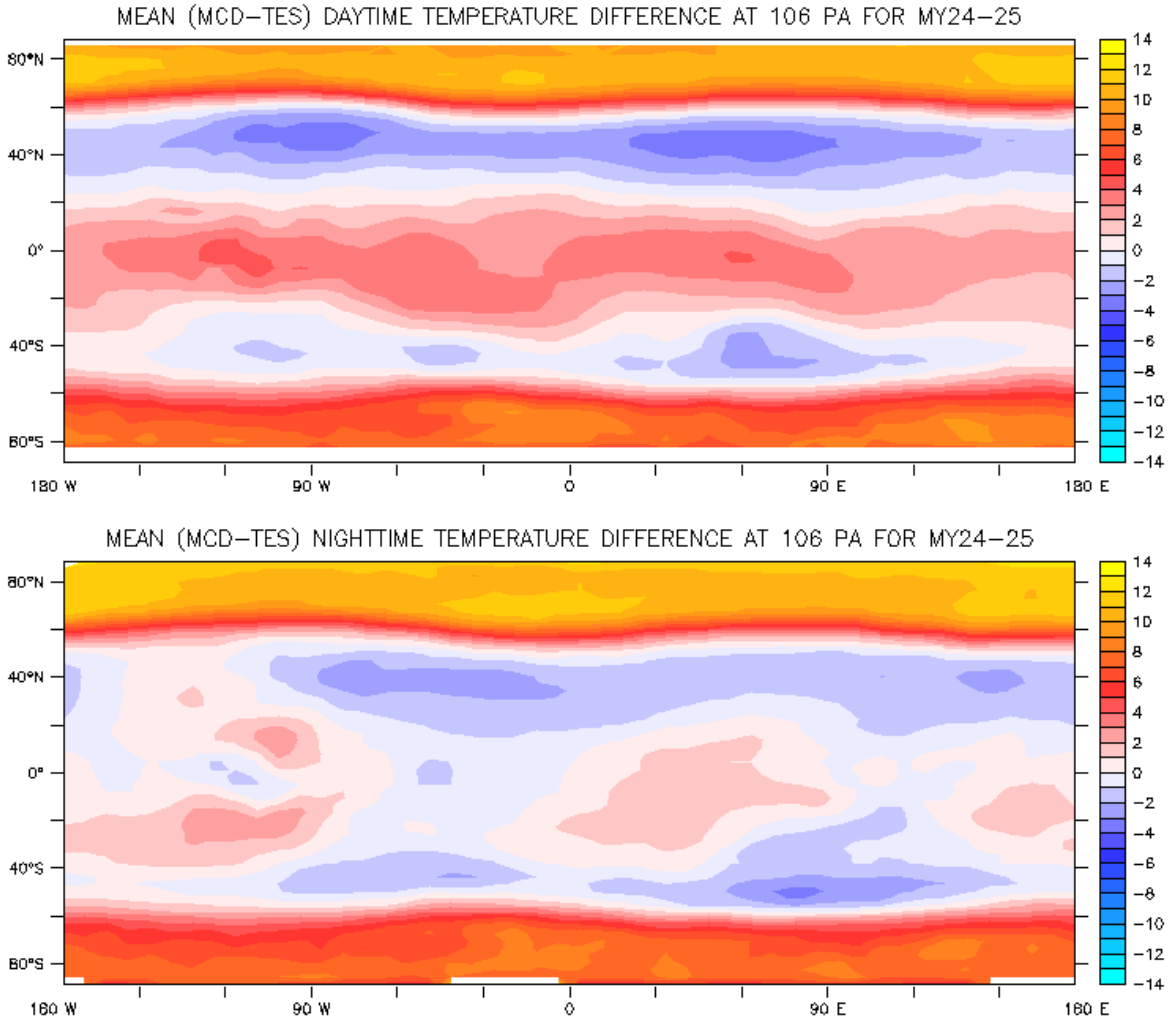

Figure 4.6 : Longitude-latitude maps of the mean (taken over time period starting at Ls=102.5 in MY24 and ending at LS=180 in MY25) difference between TES and MCD atmospheric temperature at 106 Pa. Top: Daytime (2am, local solar time) difference. Bottom: Nighttime (2pm, local solar time) difference.

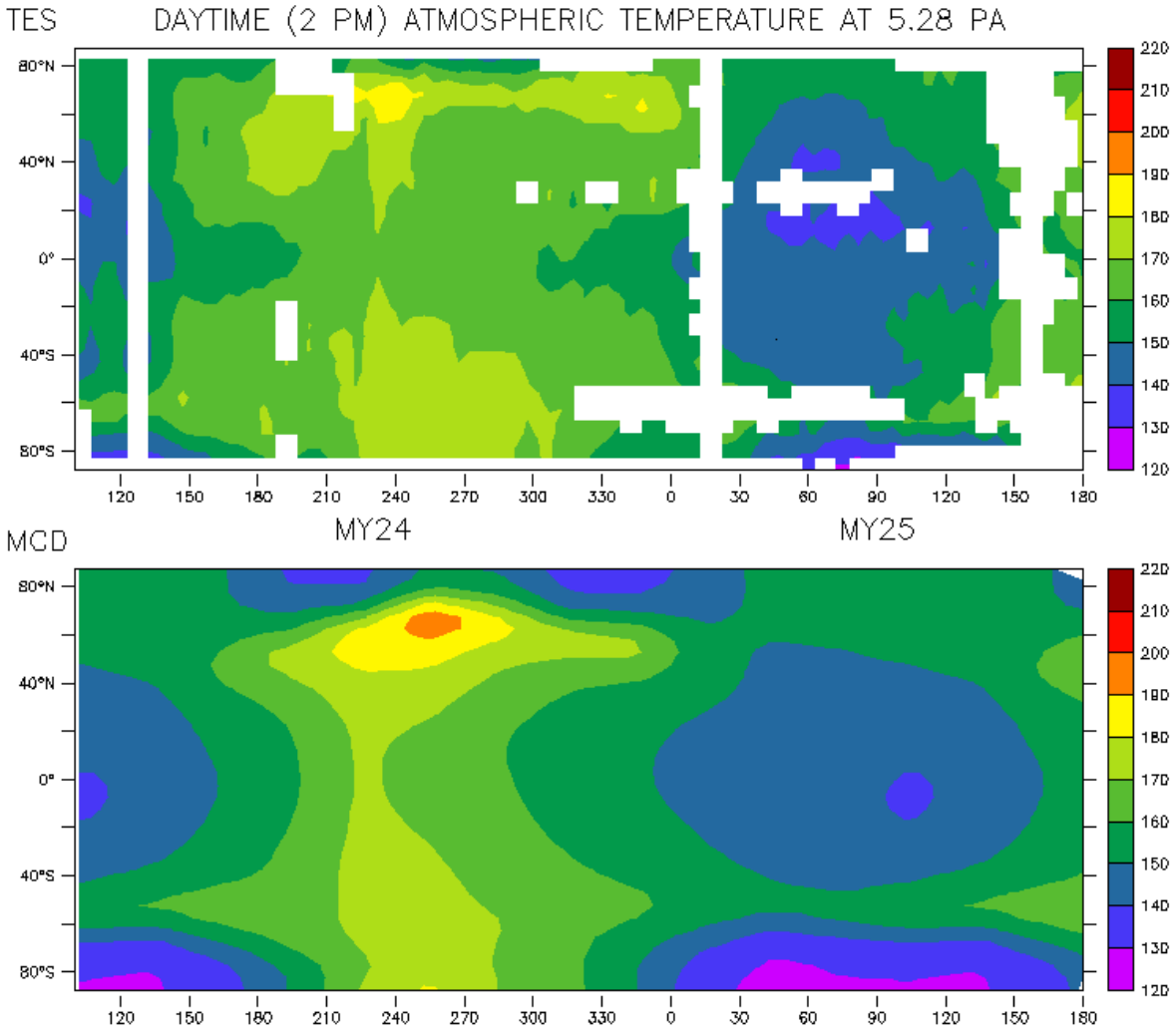

Figure 4.7 : Zonal values of atmospheric temperature at 5.28 Pa over Mars Years 24 and 25, at 2pm (local solar time). Top: TES measurements. Bottom: MCD.

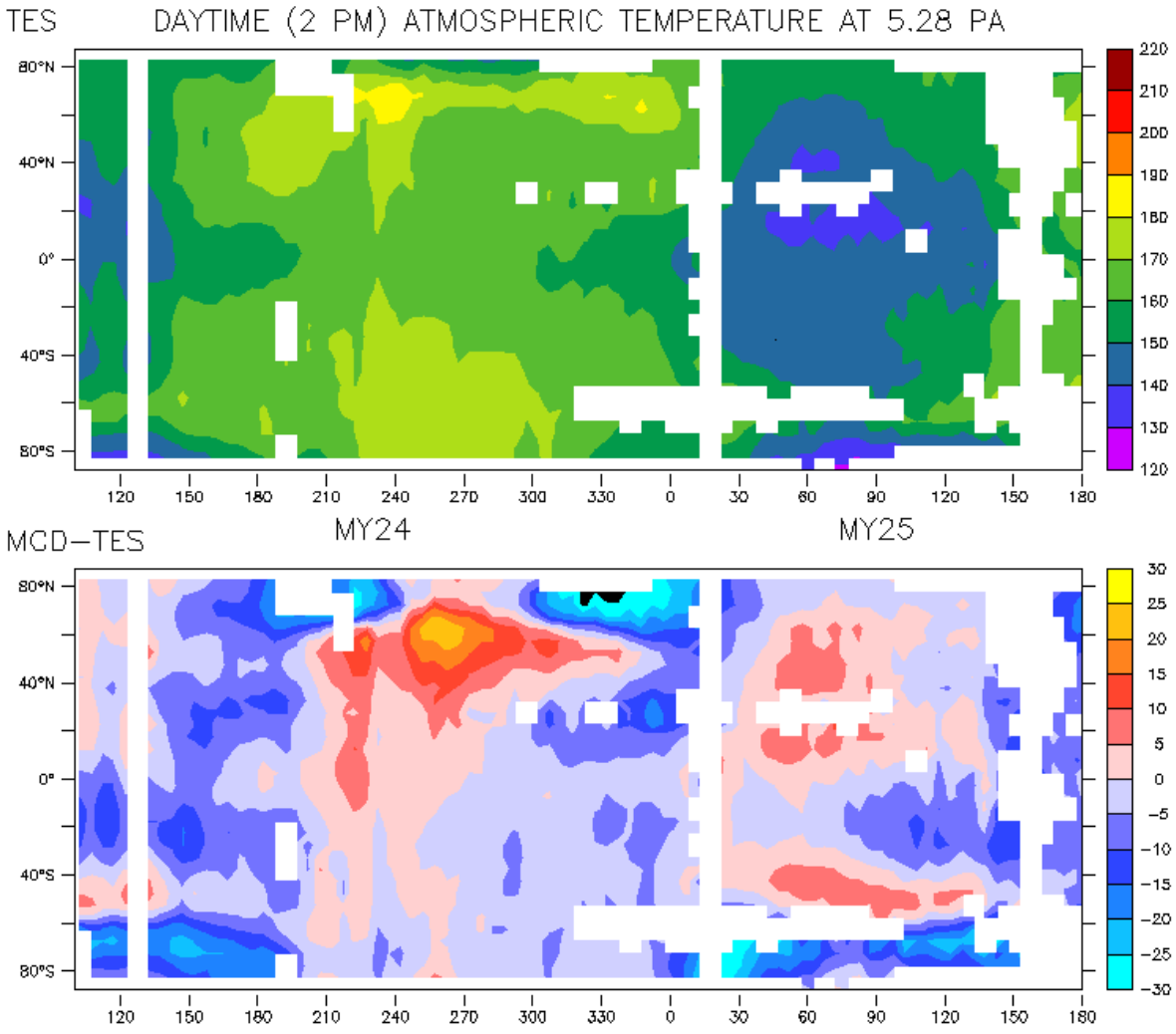

Figure 4.8 : Top : Zonal atmospheric temperature at 5.28 Pa, over Martian Years 24-25, at 2pm (local solar time) measured by TES. Bottom: Difference between MCD and TES data.

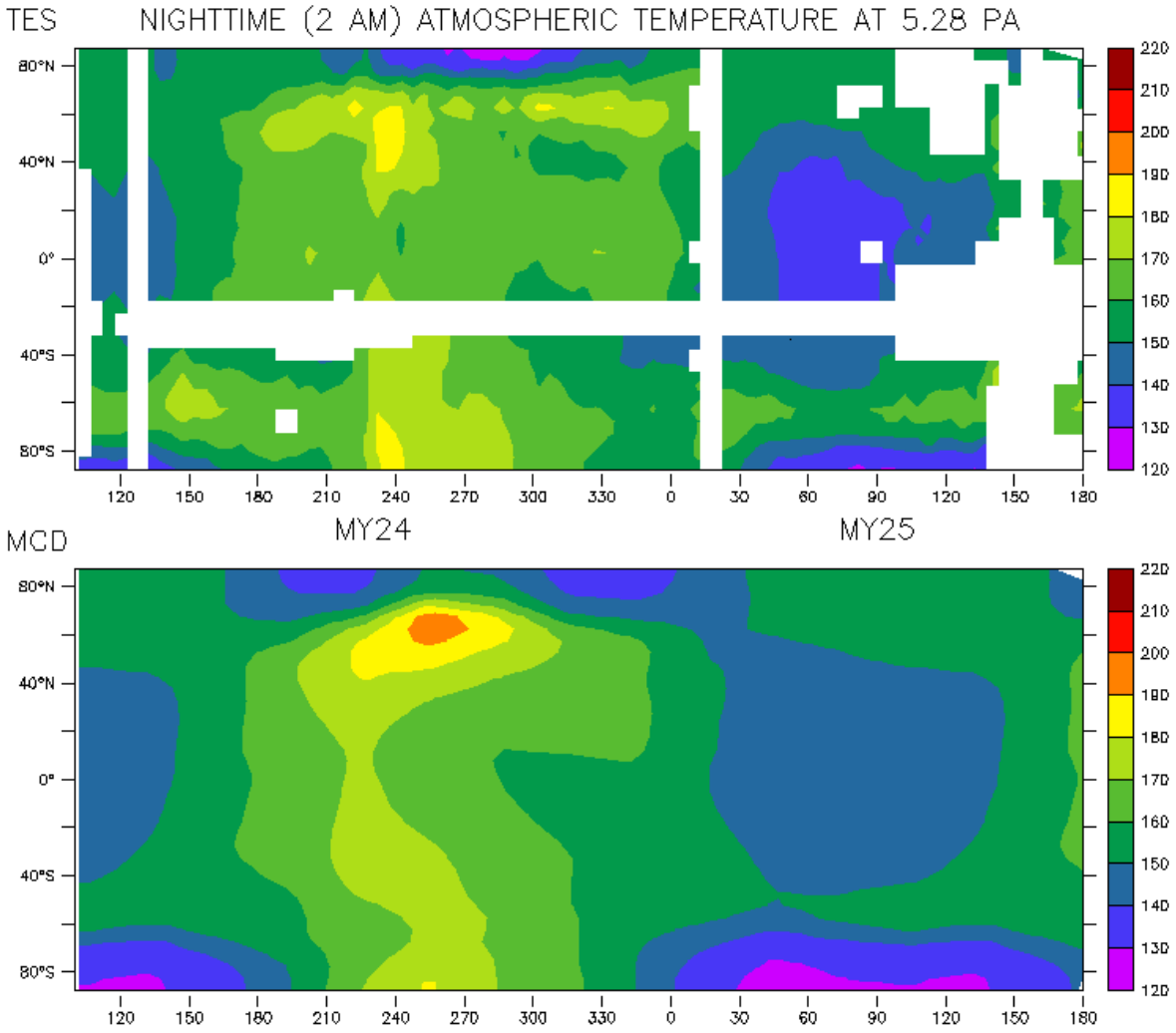

Figure 4.9 : Zonal values of atmospheric temperature at 5.28 Pa over Mars Years 24 and 25, at 2am (local solar time). Top: TES measurements. Bottom: MCD.

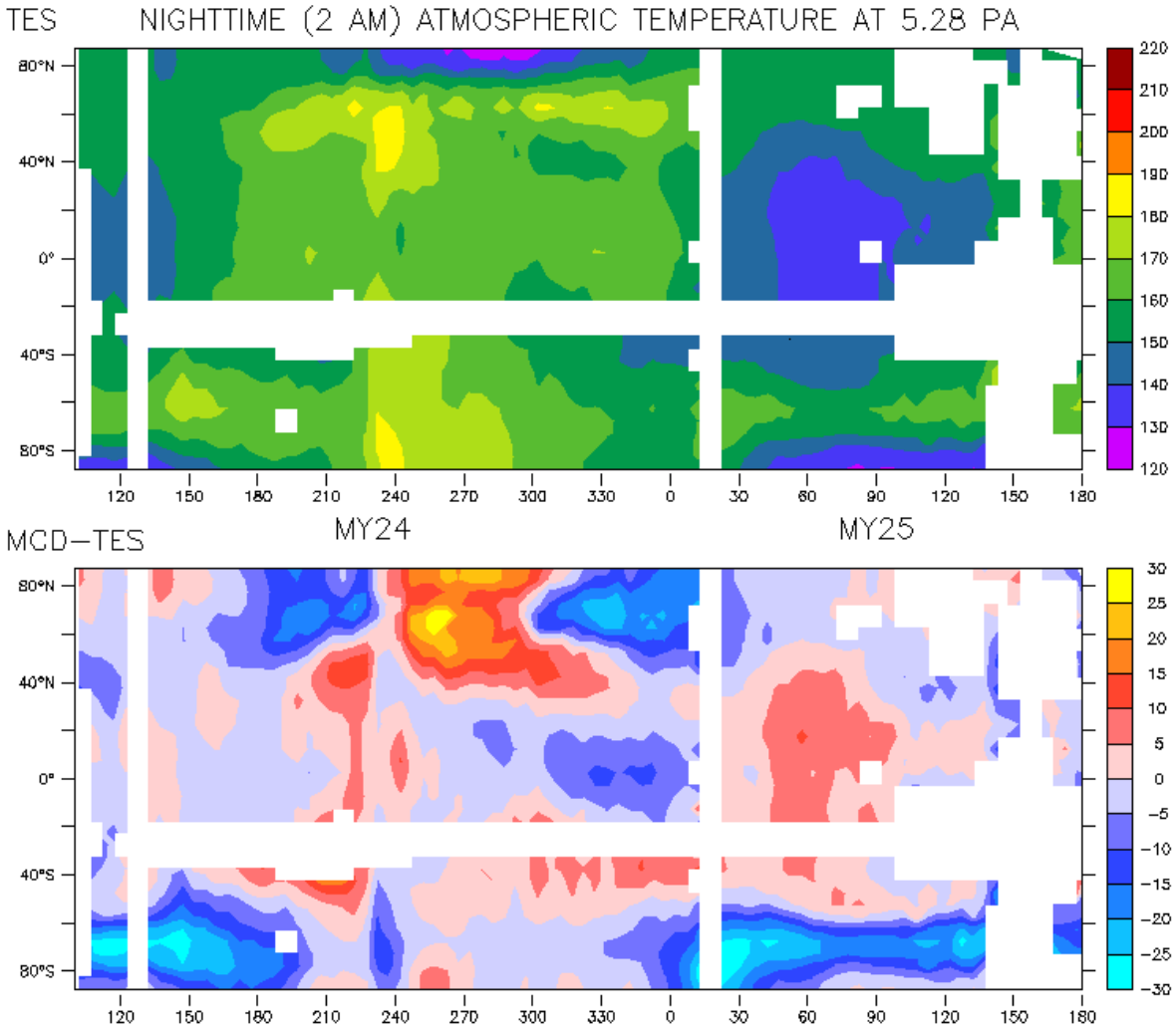

Figure 4.10 : Top : Zonal atmospheric temperature at 5.28 Pa, over Martian Years 24-25, at 2am (local solar time) measured by TES. Bottom: Difference between MCD and TES data.

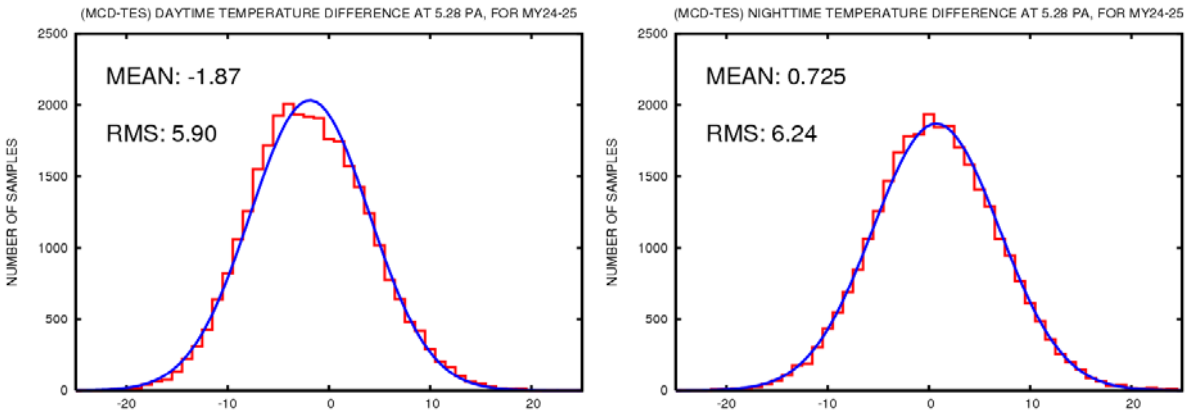

Figure 4.11 : Distribution of atmospheric temperature differences, at 5.28 Pa, between MCD and TES. Statistics were computed over Mars Years 24 and 25 (from Ls=102.5 in MY24 until Ls=180 in MY25) and for data in the [50S : 50N] latitude band, using bins of 1K. Given mean and RMS values are computed for the histograms; the blue curves are normal distributions of same mean and RMS. Left plot is for daytime data (i.e. at 2pm, local solar time) end right plot is for nighttime (i.e. 2am, local solar time) data.

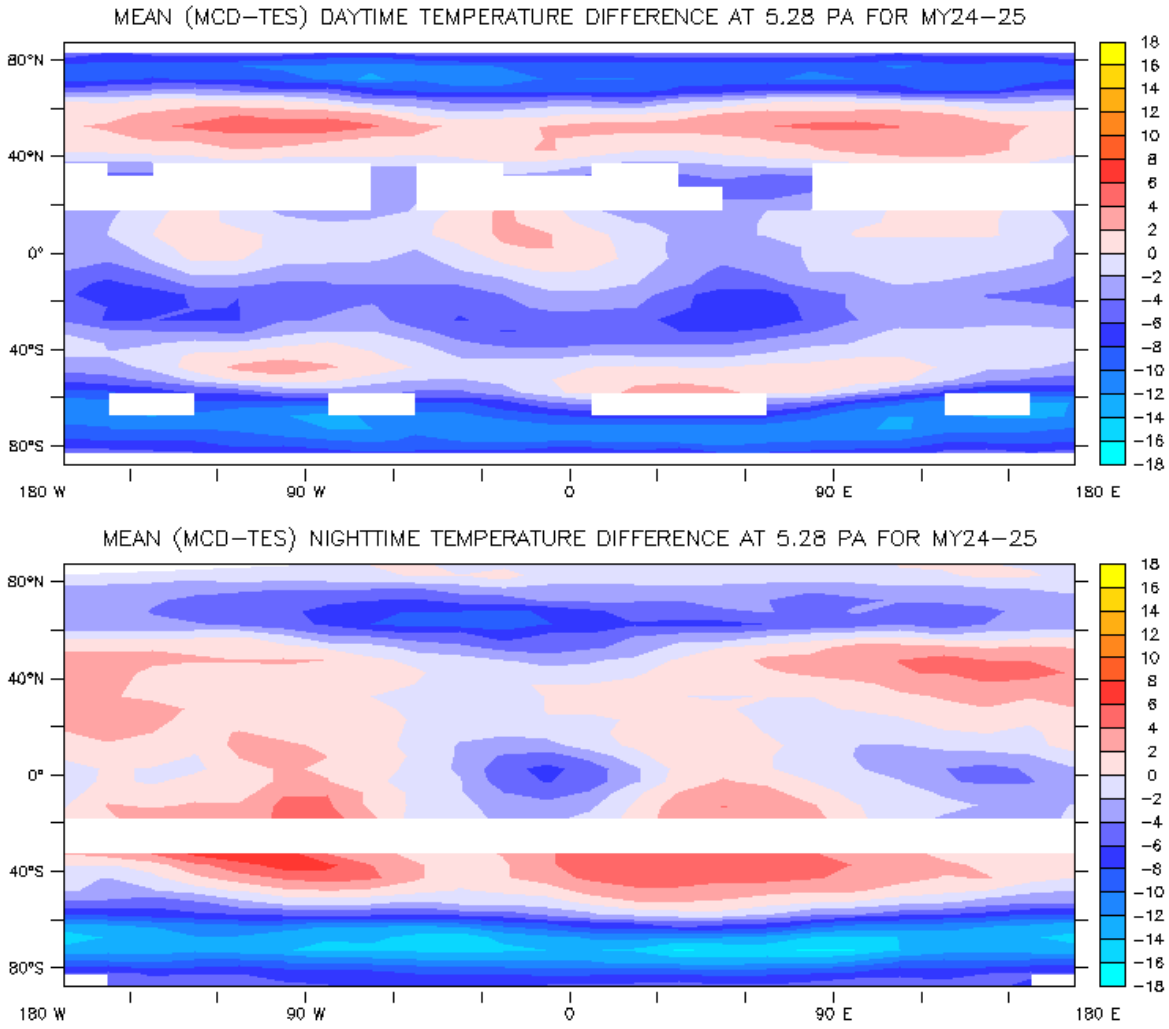

Figure 4.12 : Longitude-latitude maps of the mean (taken over time period starting at Ls=102.5 in MY24 and ending at LS=180 in MY25) difference between TES and MCD atmospheric temperature at 5.28 Pa. Top: Daytime (2am, local solar time) difference. Bottom: Nighttime (2pm, local solar time) difference.

4.1.2 Comparison using different MCD dust scenarios

Various dust scenarios are used in the MCD in order to provide atmospheres which bracket reality. This is illustrated in figure 4.13 which displays the distributions of daytime (2pm) atmospheric temperature differences (taken over time period starting at Ls=102.5 in MY24 and ending at Ls=180 in MY25) between MCD and TES at 106 Pa, when using either of MCD “MY24” (baseline), cold or warm dust scenarios.

Similarly, the capability of the MCD dust scenarios to bracket extreme events such as global dust storms is illustrated in figure 4.14: Using the MCD “warm” and “dust storm” scenarios yields colder and warmer temperature distributions than those recorded by TES during the Mars Year 25 global dust storm.

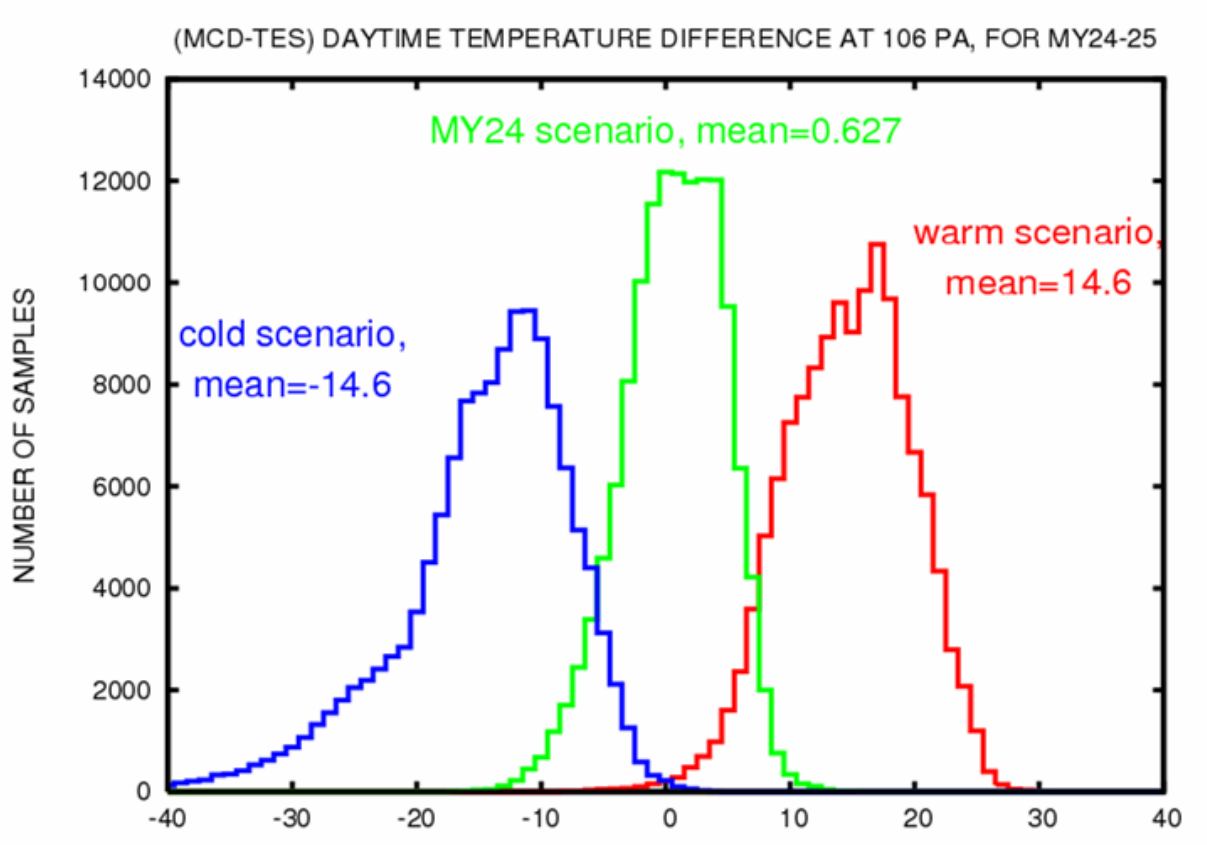

Figure 4.13 : Distributions of daytime (2pm) atmospheric temperature differences (taken over time period starting at Ls=102.5 in MY24 and ending at LS=180 in MY25) between MCD and TES at 106 Pa, within the 50S-50N latitude band, when using MCD MY24 (baseline), cold or warm dust scenarios.

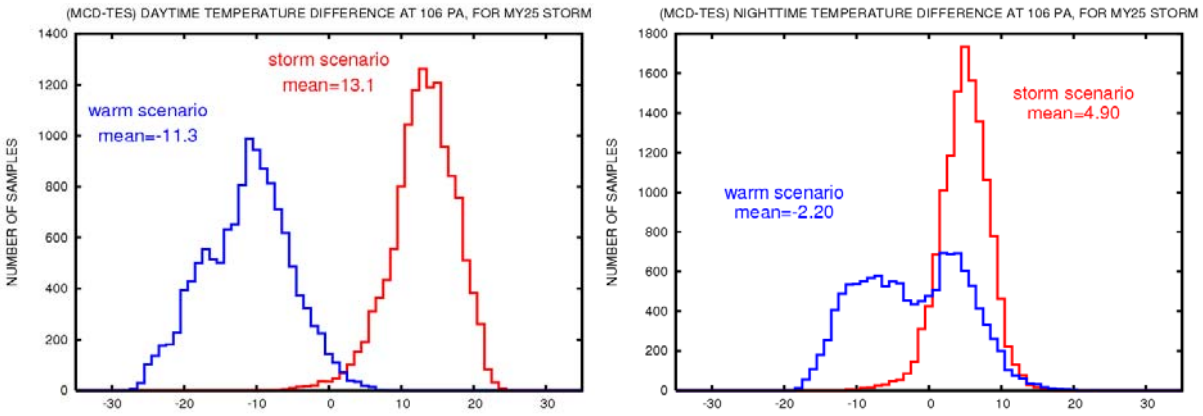

Figure 4.14 : Distributions of atmospheric temperature differences during MY25 global dust storm (from Ls=190 to Ls=230 in MY25) between MCD and TES at 106 Pa, within the 50S-50N latitude band, when using MCD "dust storm" or "warm" dust scenarios.
Left plot: daytime (2pm local solar time) differences. Right plot: nighttime (2am local solar time) differences.

4.2 Comparisons with MY26-MY27 data

Again, the comparison follows that of surface temperature comparison. As for the former, note that the existence of a large regional dust storm around Ls=320-330 in MY26 yields the most significant differences with the “MY24” baseline scenario. Nevertheless, as shown by the distributions of temperature differences between measurements and predictions, the agreement is still overall quite good.

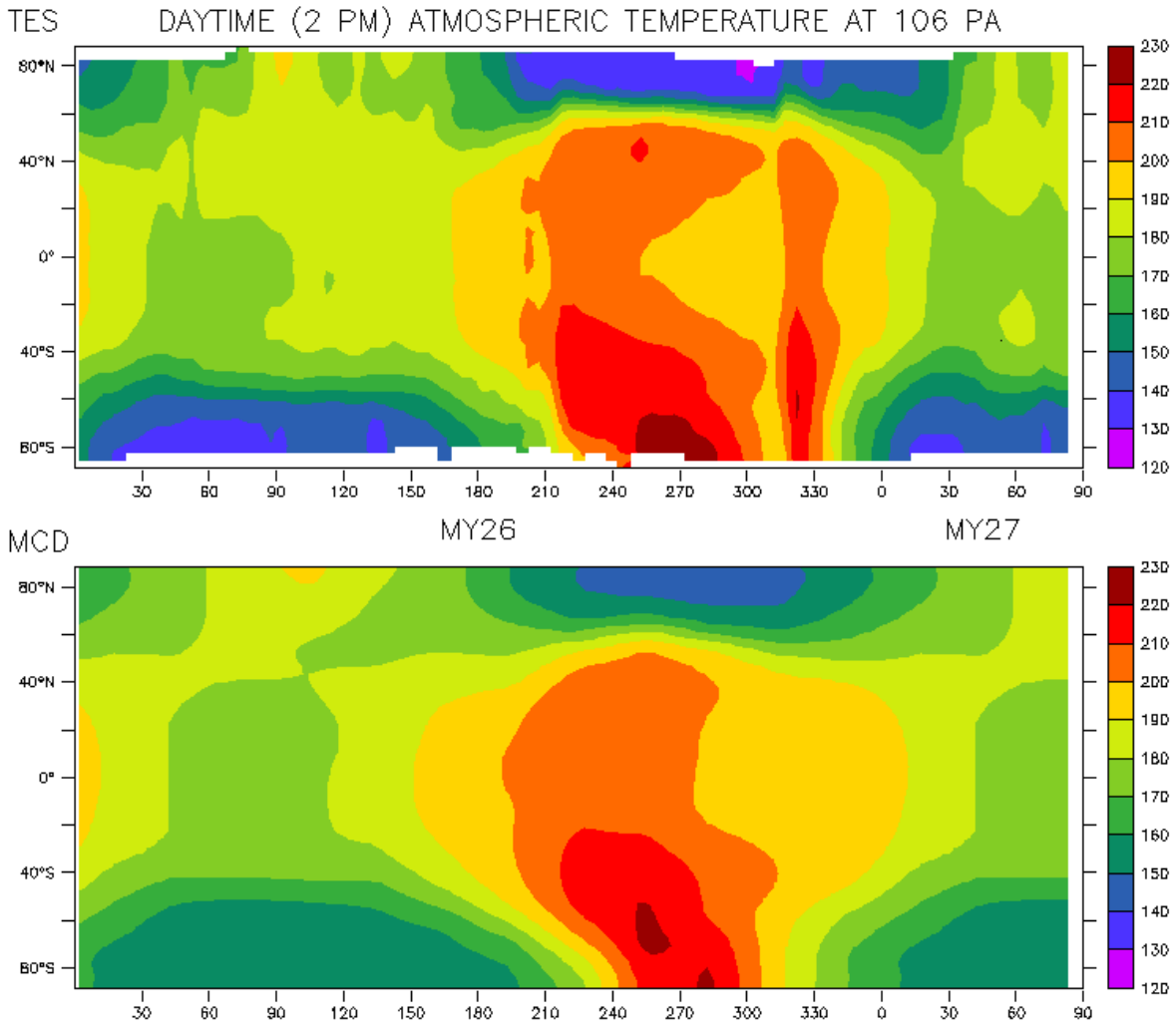

Figure 4.15 : Zonal values of atmospheric temperature at 106 Pa over Mars Years 26 and 27, at 2pm (local solar time). Top: TES measurements. Bottom: MCD.

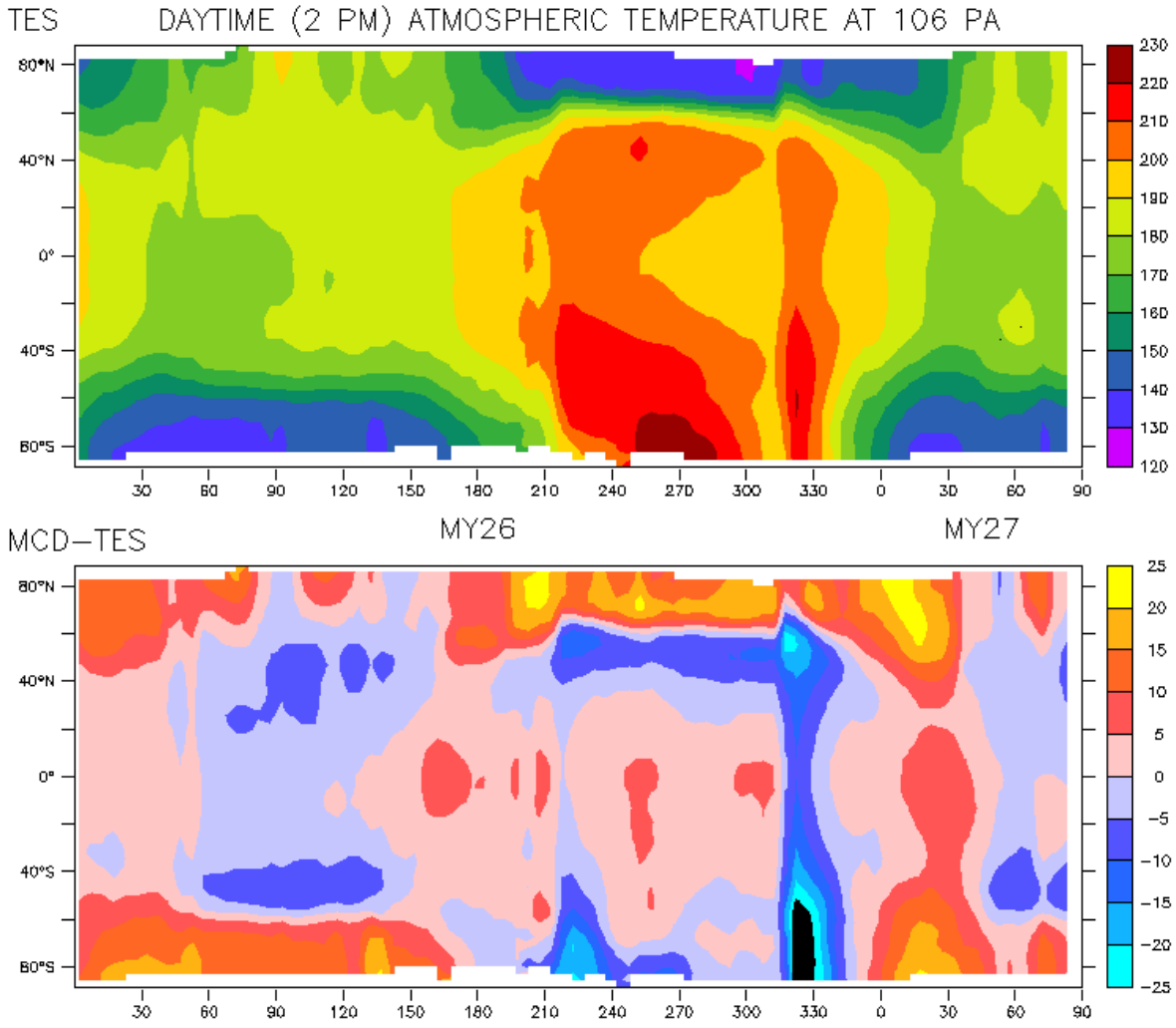

Figure 4.16 : Top : Zonal atmospheric temperature at 106 Pa, over Martian Years 26-27, at 2pm (local solar time) measured by TES. Bottom: Difference between MCD and TES data. Black regions correspond to off-scale values.

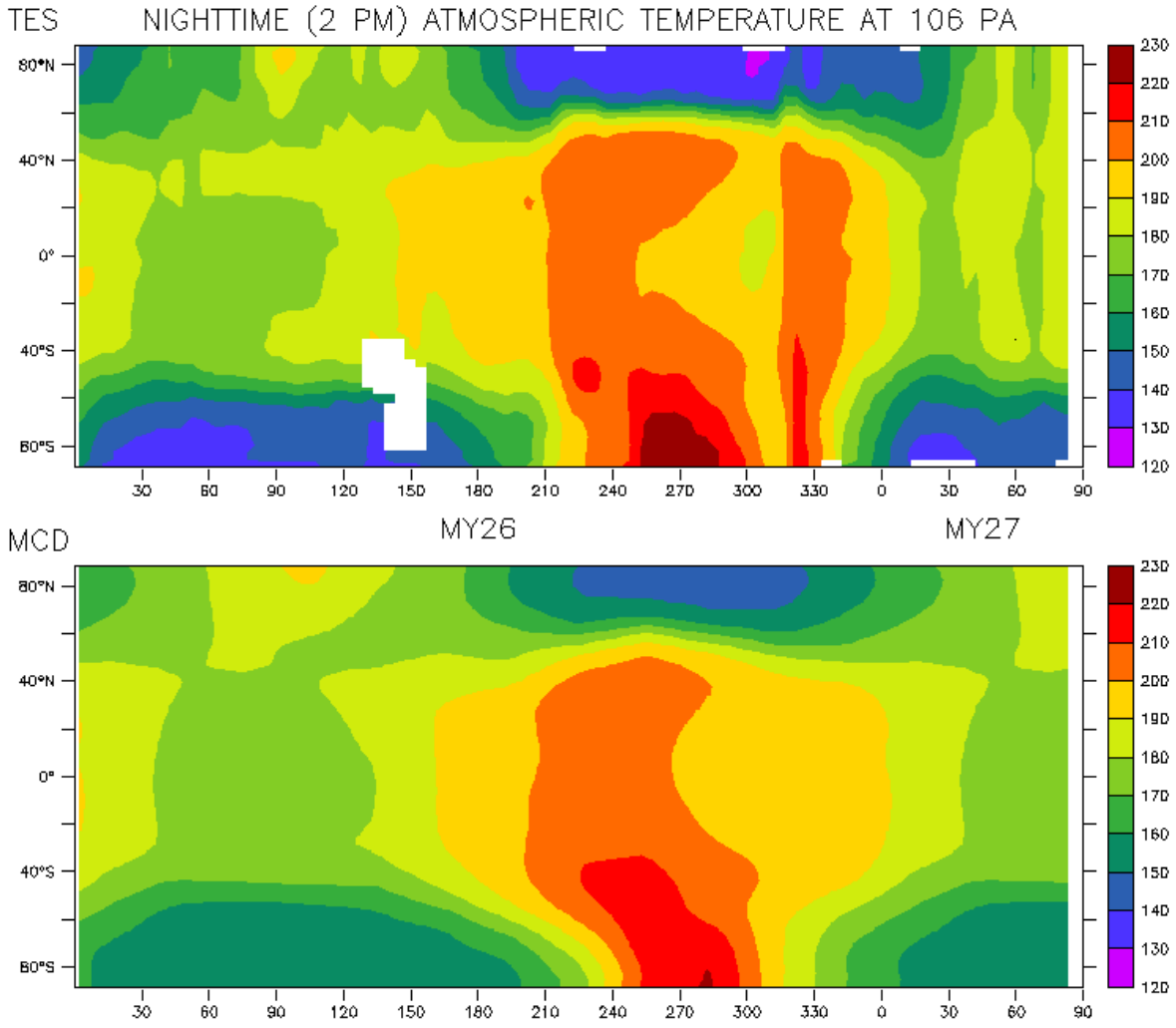

Figure 4.17 : Zonal values of atmospheric temperature at 106 Pa over Mars Years 26 and 27, at 2am (local solar time). Top: TES measurements. Bottom: MCD.

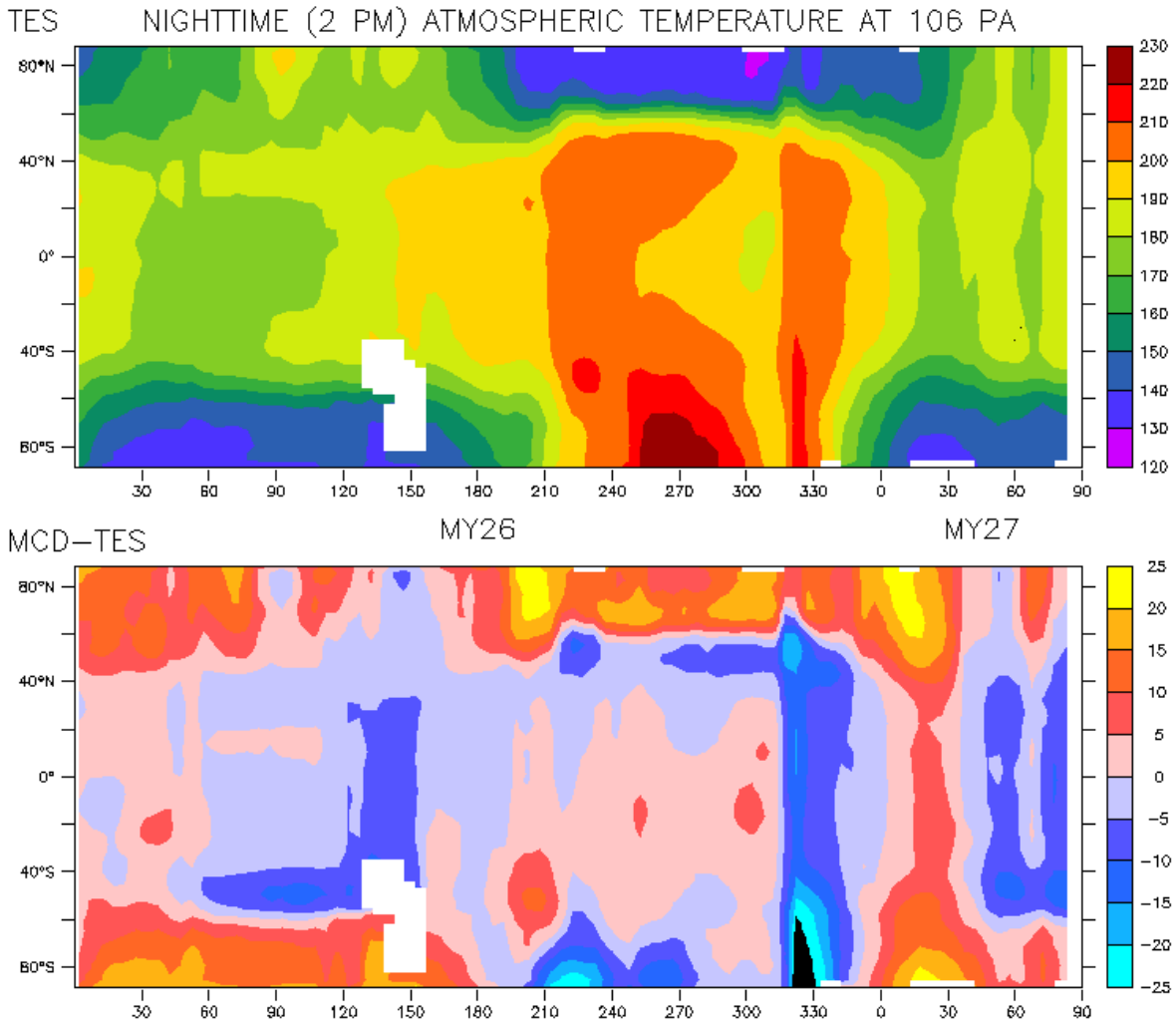

Figure 4.18 : Top : Zonal atmospheric temperature at 106 Pa, over Martian Years 26-27, at 2am (local solar time) measured by TES. Bottom: Difference between MCD and TES data. Black regions correspond to off-scale values.

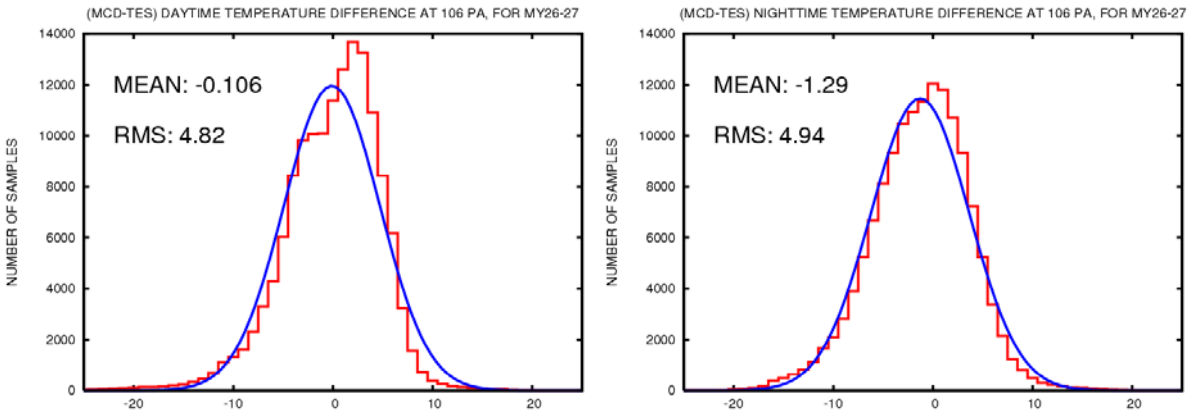

Figure 4.19 : Distribution of atmospheric temperature differences, at 106 Pa, between MCD and TES. Statistics were computed over Mars Years 26 and 27 (from Ls=0 in MY26 until Ls=85 in MY27) and for data in the [50S : 50N] latitude band, using bins of 1K. Given mean and RMS values are computed for the histograms; the blue curves are normal distributions of same mean and RMS. Left plot is for daytime data (i.e. at 2pm, local solar time) end right plot is for nighttime (i.e. 2am, local solar time) data.

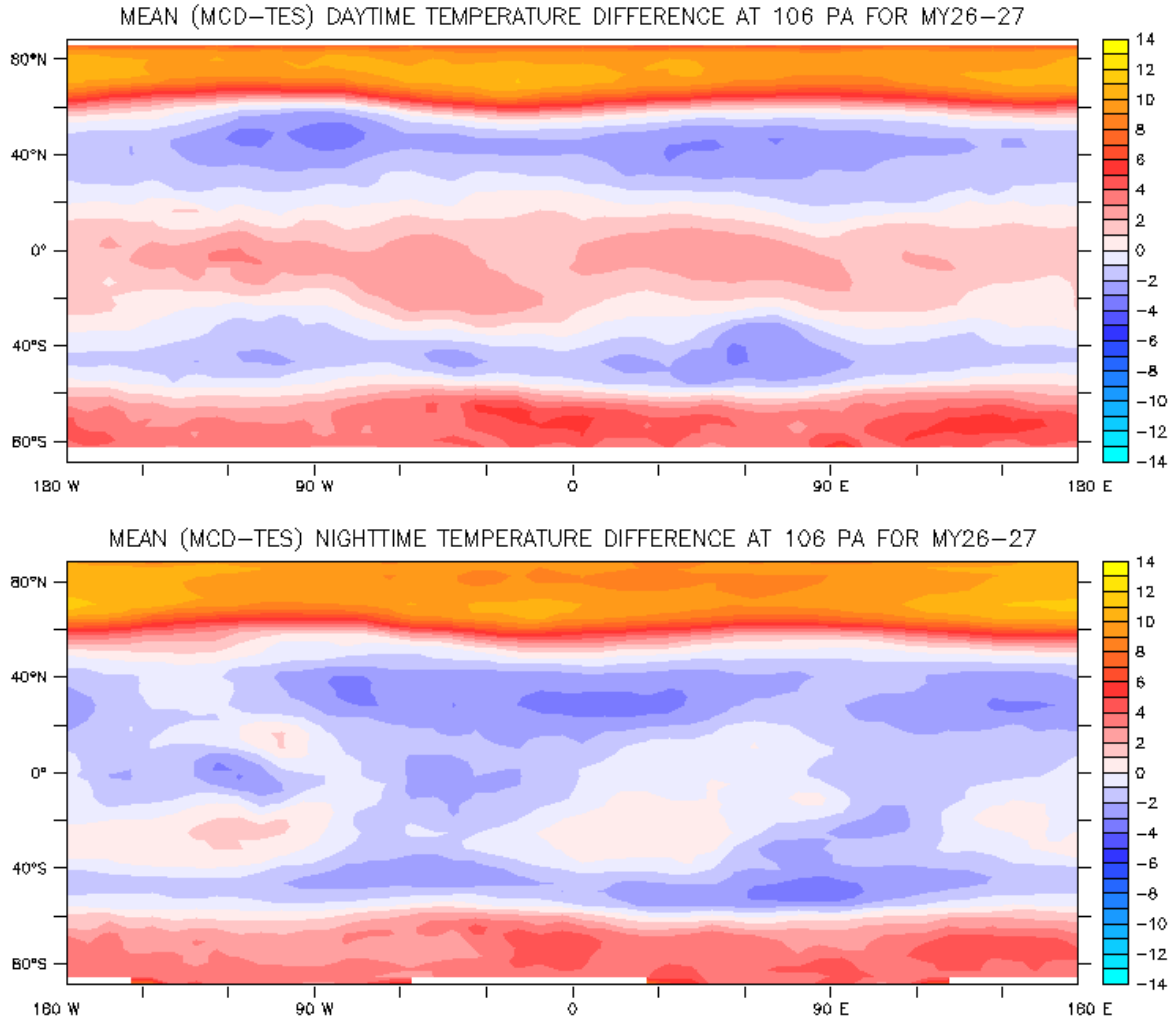

Figure 4.20 : Longitude-latitude maps of the mean (taken over time period starting at Ls=0 in MY26 and ending at Ls=85 in MY27) difference between TES and MCD atmospheric temperature at 106 Pa. Top: Daytime (2am, local solar time) difference. Bottom: Nighttime (2pm, local solar time) difference.

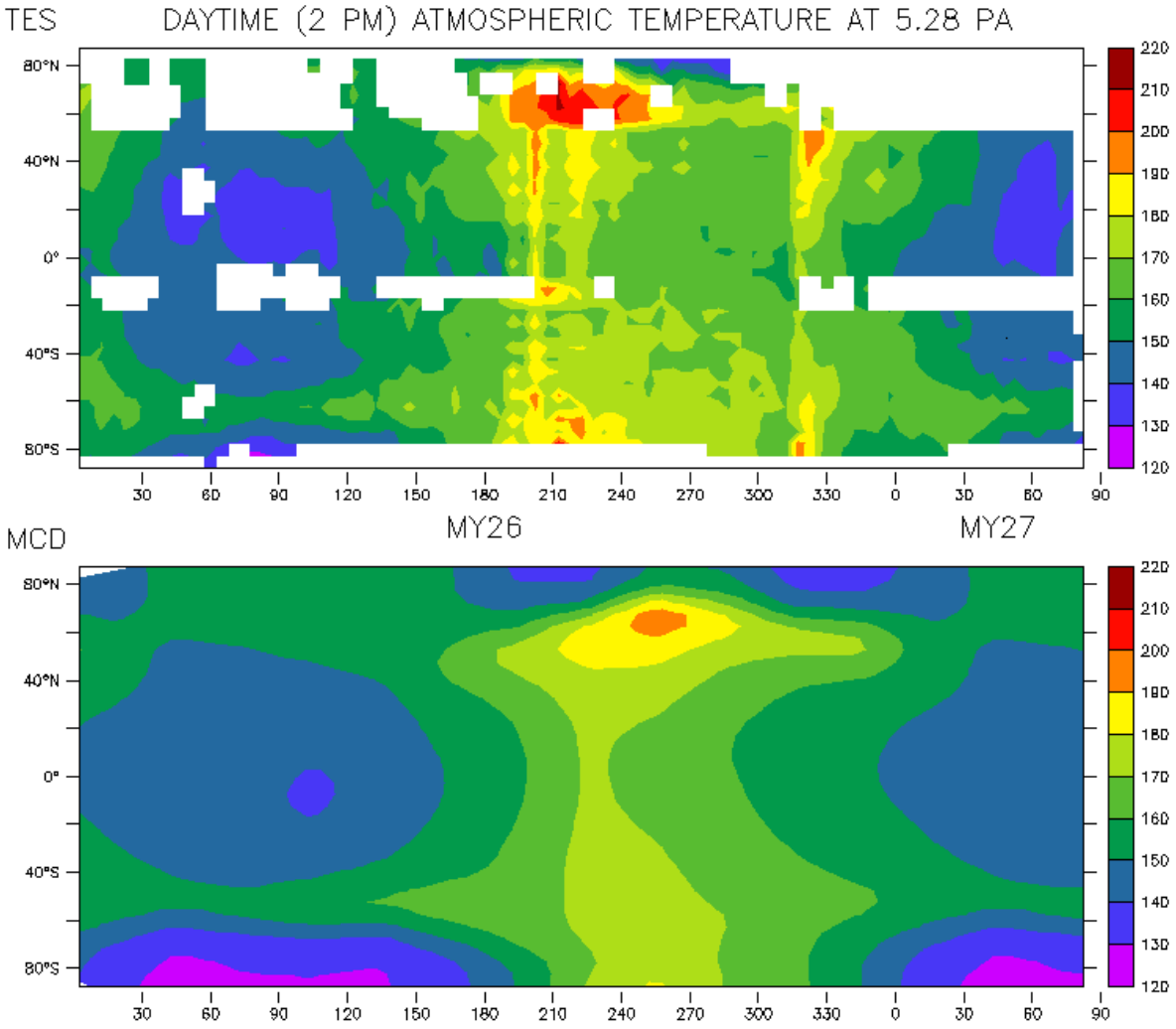

Figure 4.21 : Zonal values of atmospheric temperature at 5.28 Pa over Mars Years 26 and 27, at 2pm (local solar time). Top: TES measurements. Bottom: MCD.

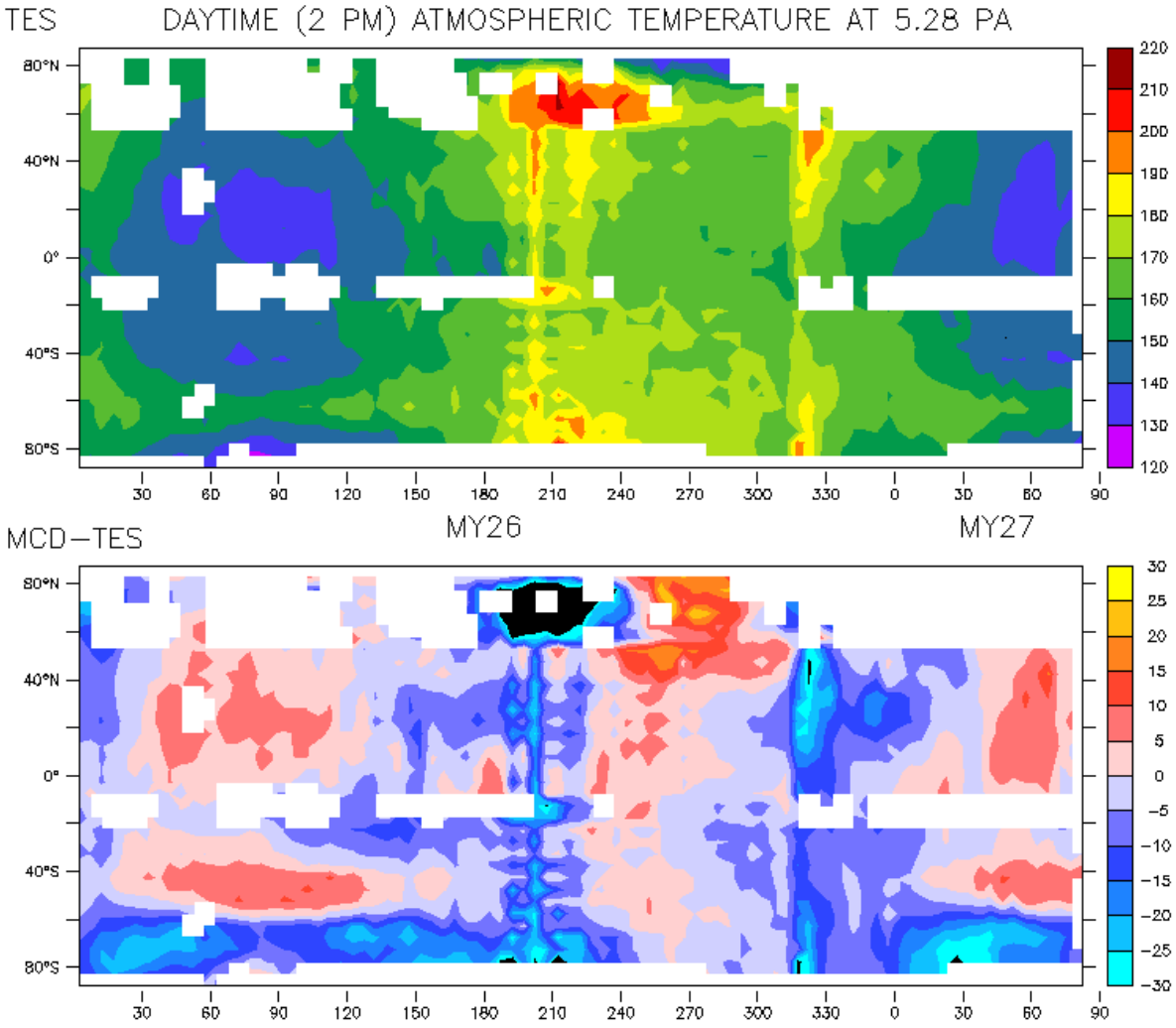

Figure 4.22 : Top : Zonal atmospheric temperature at 5.28 Pa, over Martian Years 26-27, at 2pm (local solar time) measured by TES. Bottom: Difference between MCD and TES data. Black regions correspond to off-scale values.

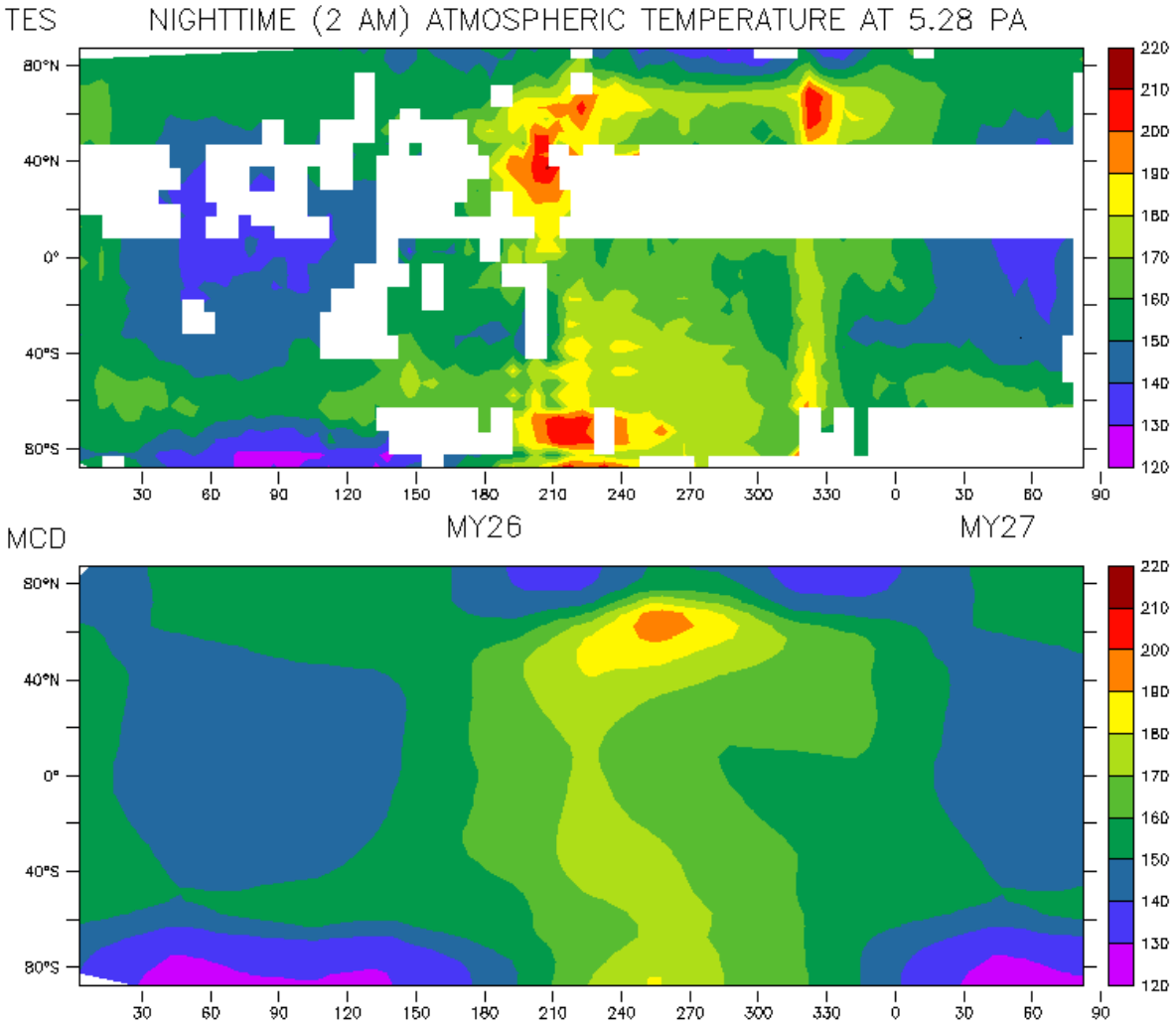

Figure 4.23 : Zonal values of atmospheric temperature at 5.28 Pa over Mars Years 26 and 27, at 2am (local solar time). Top: TES measurements. Bottom: MCD.

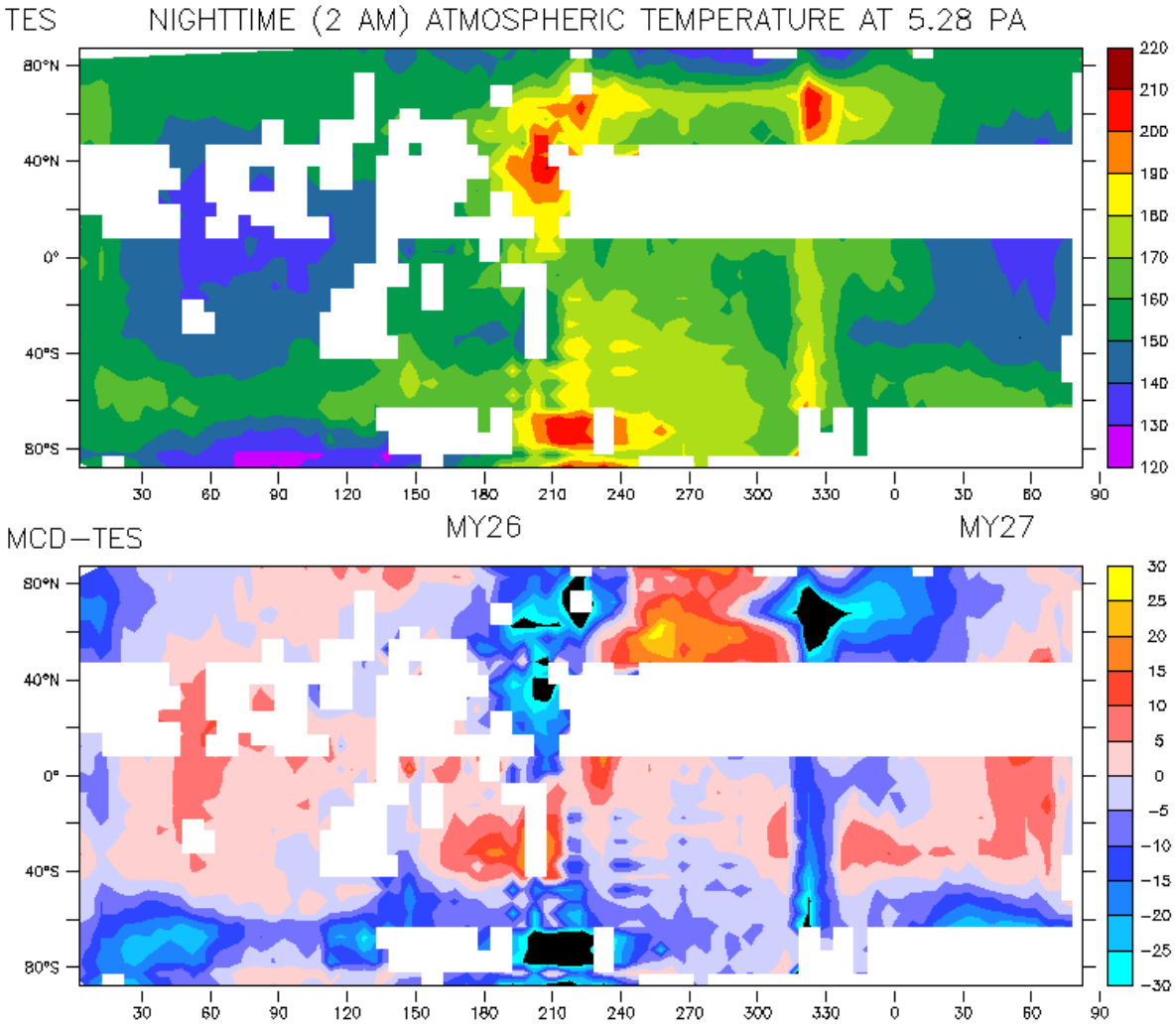

Figure 4.24 : Top : Zonal atmospheric temperature at 5.28 Pa, over Martian Years 26-27, at 2am (local solar time) measured by TES. Bottom: Difference between MCD and TES data. Black regions correspond to off-scale values.

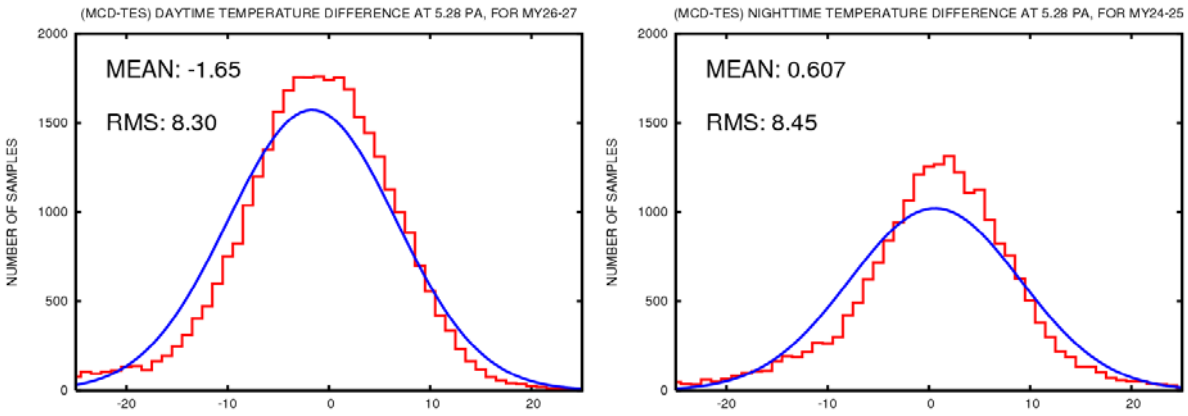

Figure 4.25 : Distribution of atmospheric temperature differences, at 5.28 Pa, between MCD and TES. Statistics were computed over Mars Years 26 and 27 (from Ls=0 in MY26 until Ls=85 in MY27) and for data in the [50S : 50N] latitude band, using bins of 1K. Given mean and RMS values are computed for the histograms; the blue curves are normal distributions of same mean and RMS. Left plot is for daytime data (i.e. at 2pm, local solar time) end right plot is for nighttime (i.e. 2am, local solar time) data.

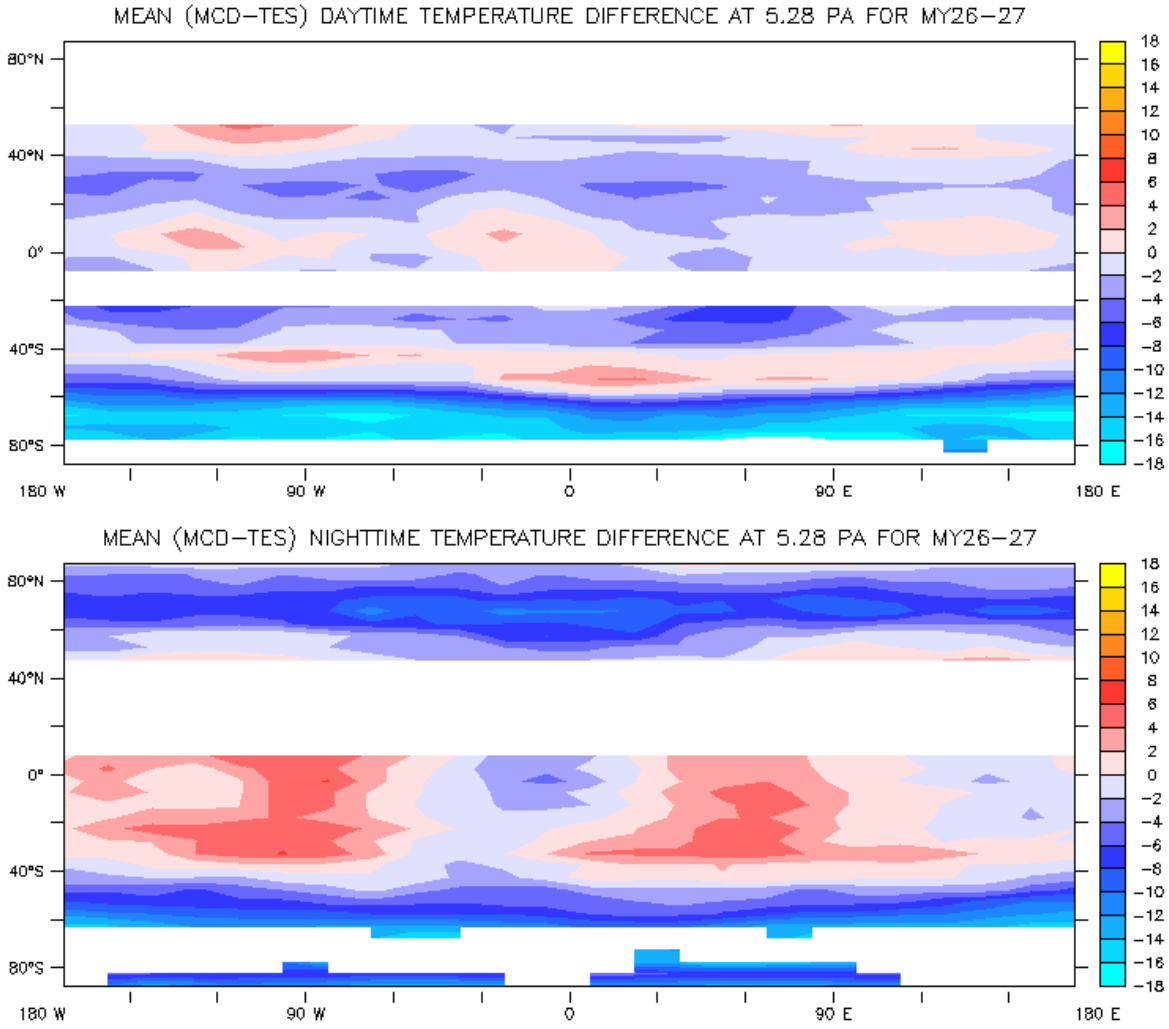

Figure 4.26 : Longitude-latitude maps of the mean (taken over time period starting at Ls=0 in MY26 and ending at Ls=85 in MY27) difference between TES and MCD atmospheric temperature at 5.28 Pa. Top: Daytime (2am, local solar time) difference. Bottom: Nighttime (2pm, local solar time) difference.

5. Surface pressure comparisons

The high resolution mode of the MCD includes a surface pressure predictor which combine informations from a high resolution topography map (1/32 deg res.) from the MGS MOLA experiment (to account for the local topography variations), the Mars climate database pressure maps (to account for the dynamical pressure gradients and tides) and the smoothed Viking Lander 1 pressure records (used as a reference point to correct the atmospheric mass).
The tool can be tested by comparing its prediction where pressure records are available in addition to Viking Lander 1 : Viking Lander 2 and Pathfinder.

5.1 Comparison with Viking Lander 2 records

Viking Lander 2 recorded surface pressure for over two years. This record provides a good test to check model results against.

Figure 5.1 shows the evolution of (diurnaly averaged) surface pressure over a year which includes the 1977 global dust storm which affected the thermal structure, the atmospheric dynamics and, in turn, the pressure at mid-latitudes.
By using the appropriate dust scenario (baseline “MY24” for most of the year and “dust storm” during the 1977 storm), the correct surface pressure is predicted.

The variability of surface pressure with seasons, as obtained by the MCD, also compares well with recorded values, as shown in Figure 5.2

5.2 Comparison with Pathfinder records

Pathfinder recorded very frequently and almost continuously surface pressure during 30 sols after its landing (ie: for Ls=142 to Ls=158, in Mars Year 23). Figure 5.3 displays the measured diurnal cycle along with values predicted by the “cold”, “warm” and baseline “MY24” scenarios at the same location.
Although the overall trends and variations with time of day are well represented, there is an overall net 20 Pa shift between datasets.This shift is not well understood. It could results from:

- A change in atmospheric mass between the time observed by Viking 1 (our reference point) and Pathfinder
- A difference in absolute calibration between Viking and Pathfinder
- A bias due to the model. However, Pathfinder and Viking are not very distant. The bias is observed when the 2 dataset are simply interpolated and compared....

Observations by Phoenix starting in May 2008 should help solve the discrepancy.

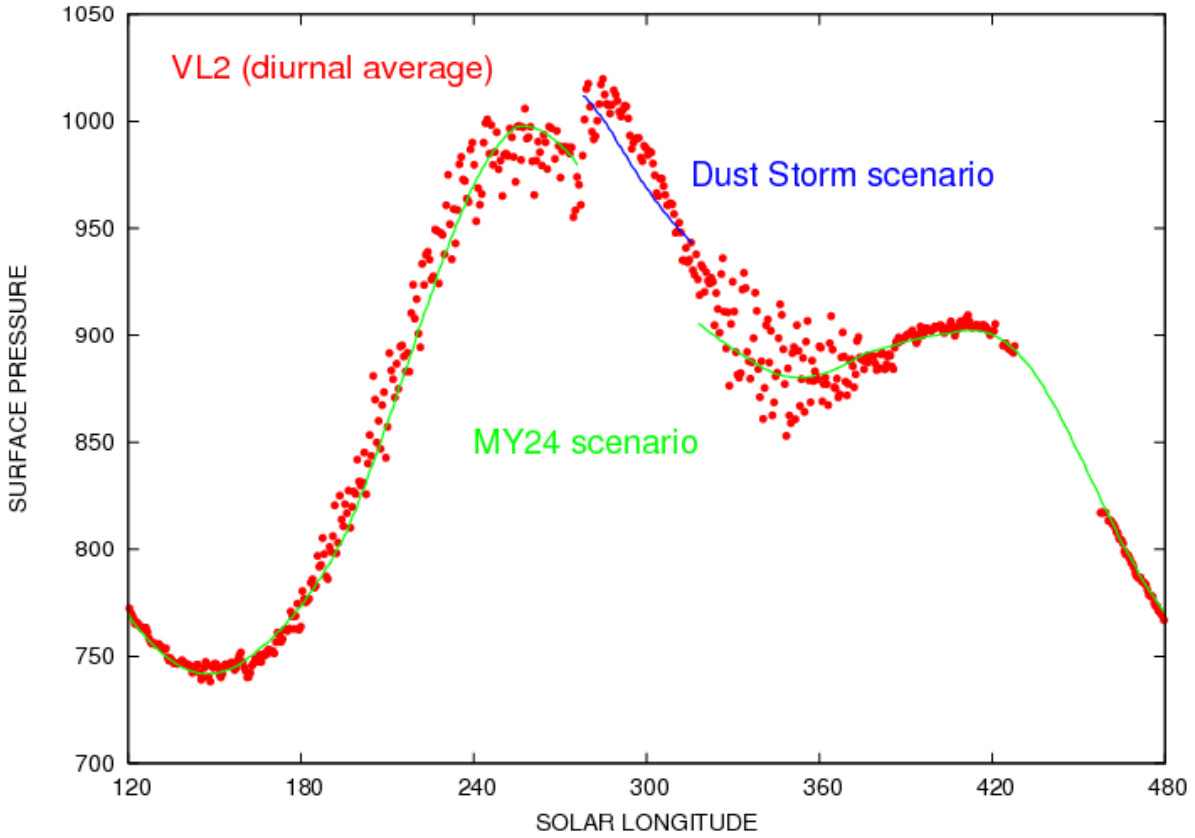

Figure 5.1 : Surface pressure (in Pa) recorded by Viking Lander 2 (red dots) and MCD predictions using the baseline "MY24" scenario (green line) and "dust storm" scenario (blue line). Switching from one to the other enables to recover the change in behaviour recorded by VL2 during the 1977 global dust storm.

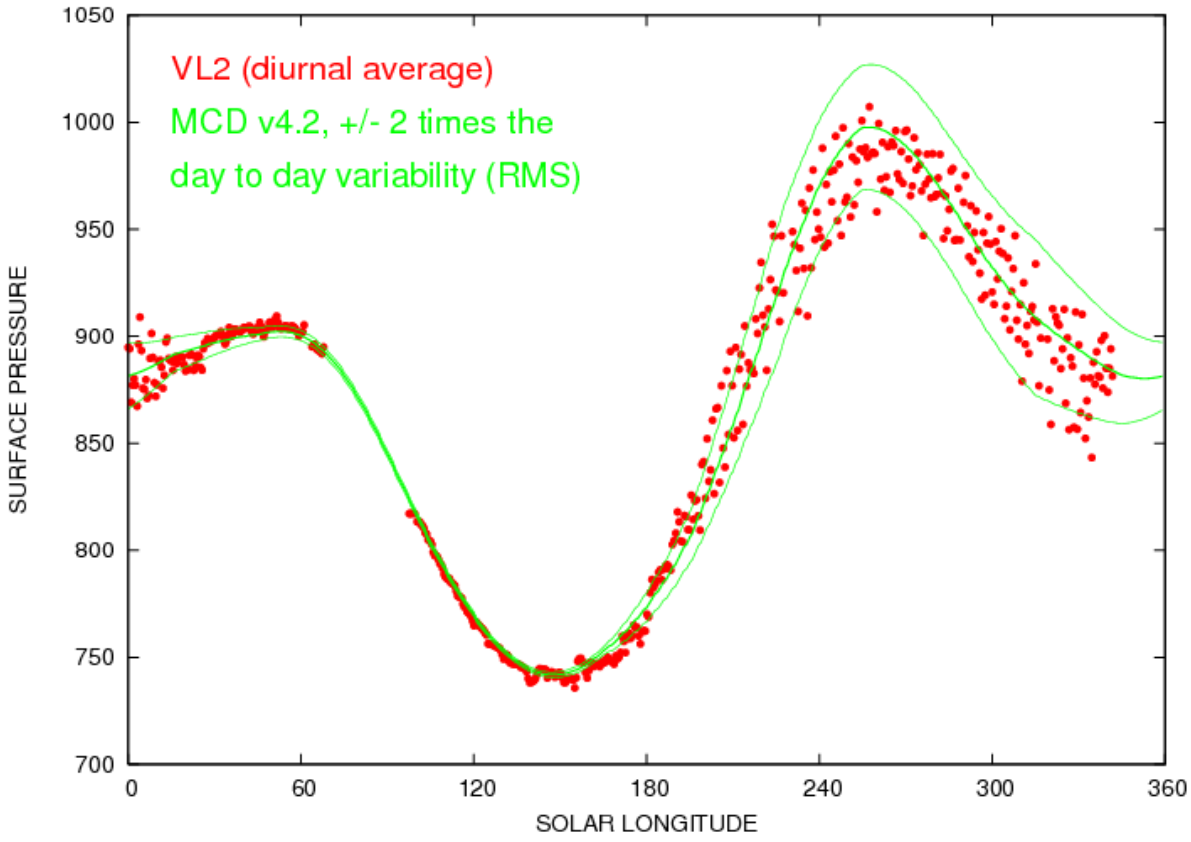

Figure 5.2 : Surface pressure cycle over a Martian year, as predicted by the baseline "MY24" scenario at Viking Lander 2 site, with an envelope of twice its standard deviation, compared to recorded values.

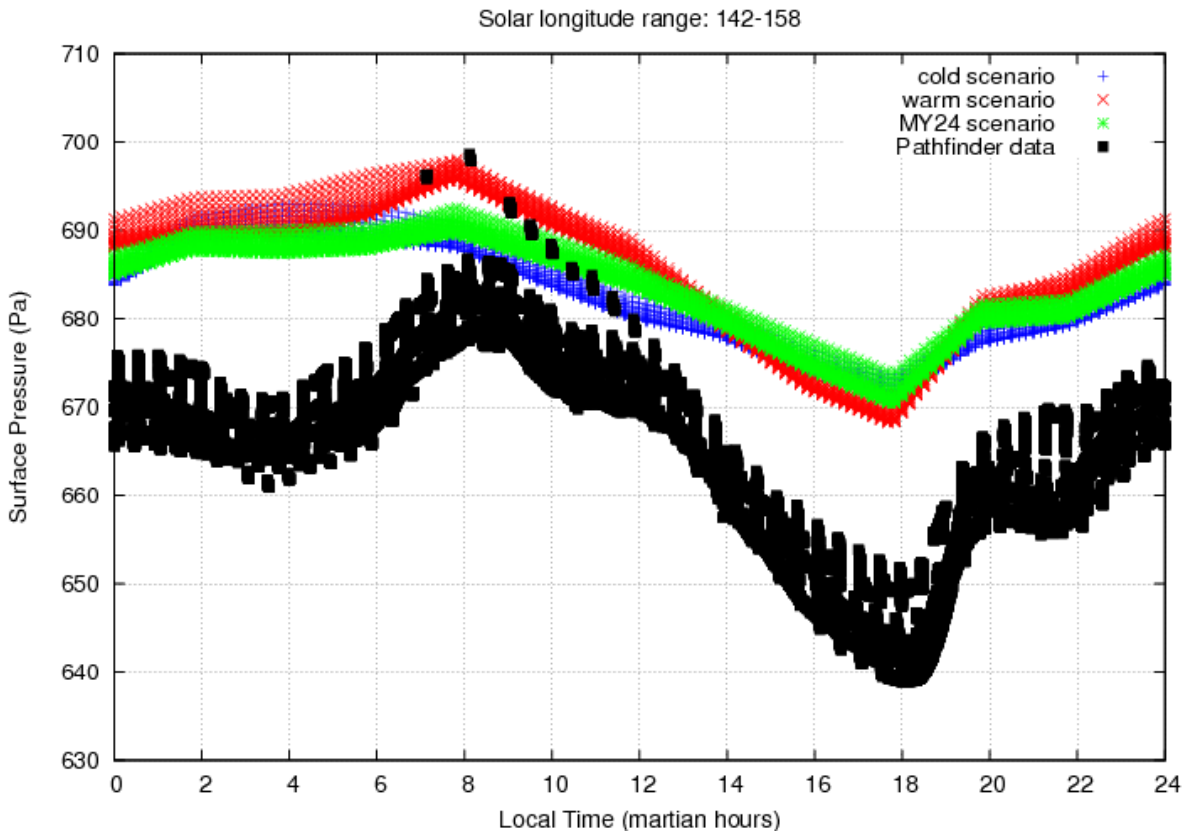

Figure 5.3 : Surface pressure diurnal cycle, as measured by Pathfinder during 30 sols (from Ls=142 to Ls=158, in Mars Year 23) and predicted by the “cold”, “warm” and baseline “MY24” scenarios at the same location.

6. Comparisons with Opportunity entry profile

Opportunity landed in Mars Year 26 (at Ls=339). Atmospheric temperature during its descent was retrieved by P.Withers. Note that at that time Mars Express and TES have shown that the atmosphere was dustier than usual, which fits well with MCD predictions displayed in figure 6.1.

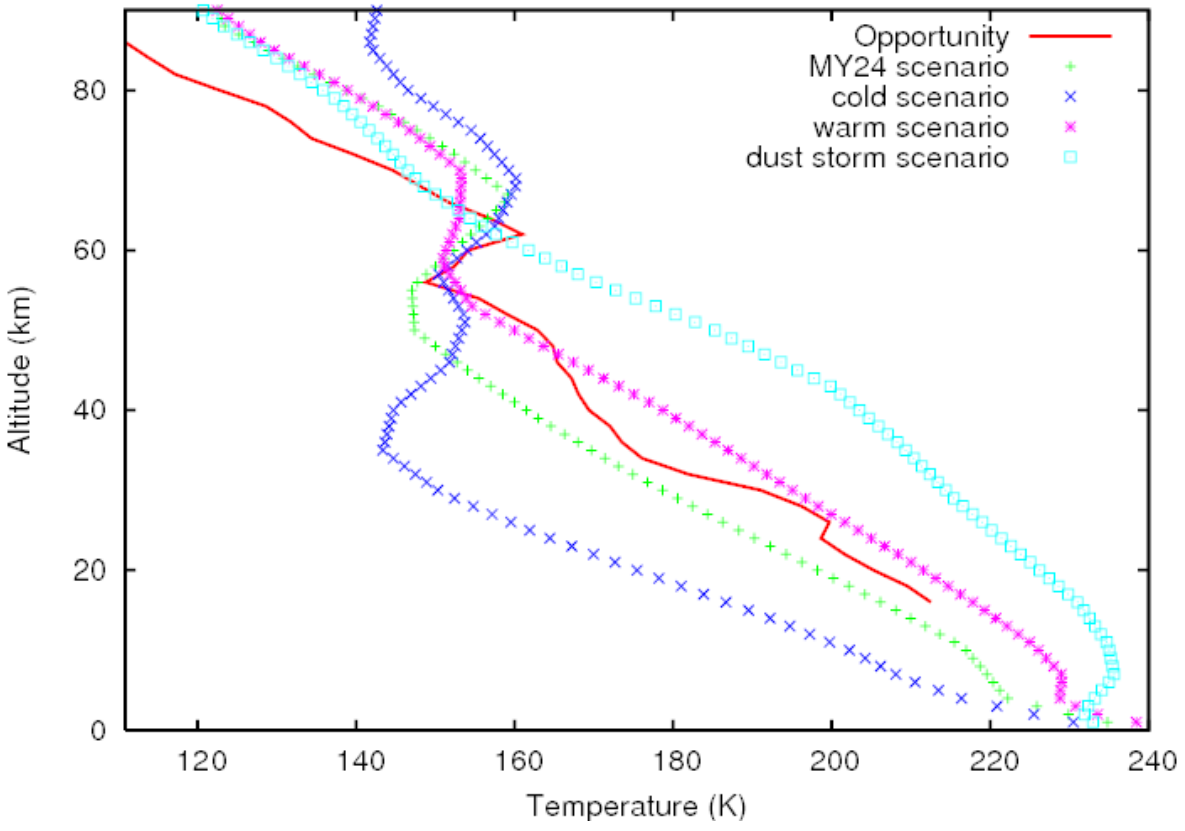

Figure 6.1 : Opportunity entry temperature profile (retrieved by P. Withers) compared to the MCD predictions for the various dust scenarios.

7. Comparisons with TES Water Vapour Column

TES data acquisition enabled to derive the water vapour column and provide datasets for comparison. Again values can be compared during MY24 and MY25 (global dust storm exclude) as well as MY26 and MY27.

Zonal distributions of water vapour columns measured by TES and predicted by the MCD, as wall as distributions of MCD-TES differences are given in figures 7.1 to 7.6. Note that the trends are qualitatively well represented, but that values given by the MCD are overall too wet. This can however be traced back to the fact that some elements of the Global Circulation Model (from which the MCD is derived) was tuned using earlier (much wetter and revised since) TES data, as shown in figures 7.3 and 7.6.

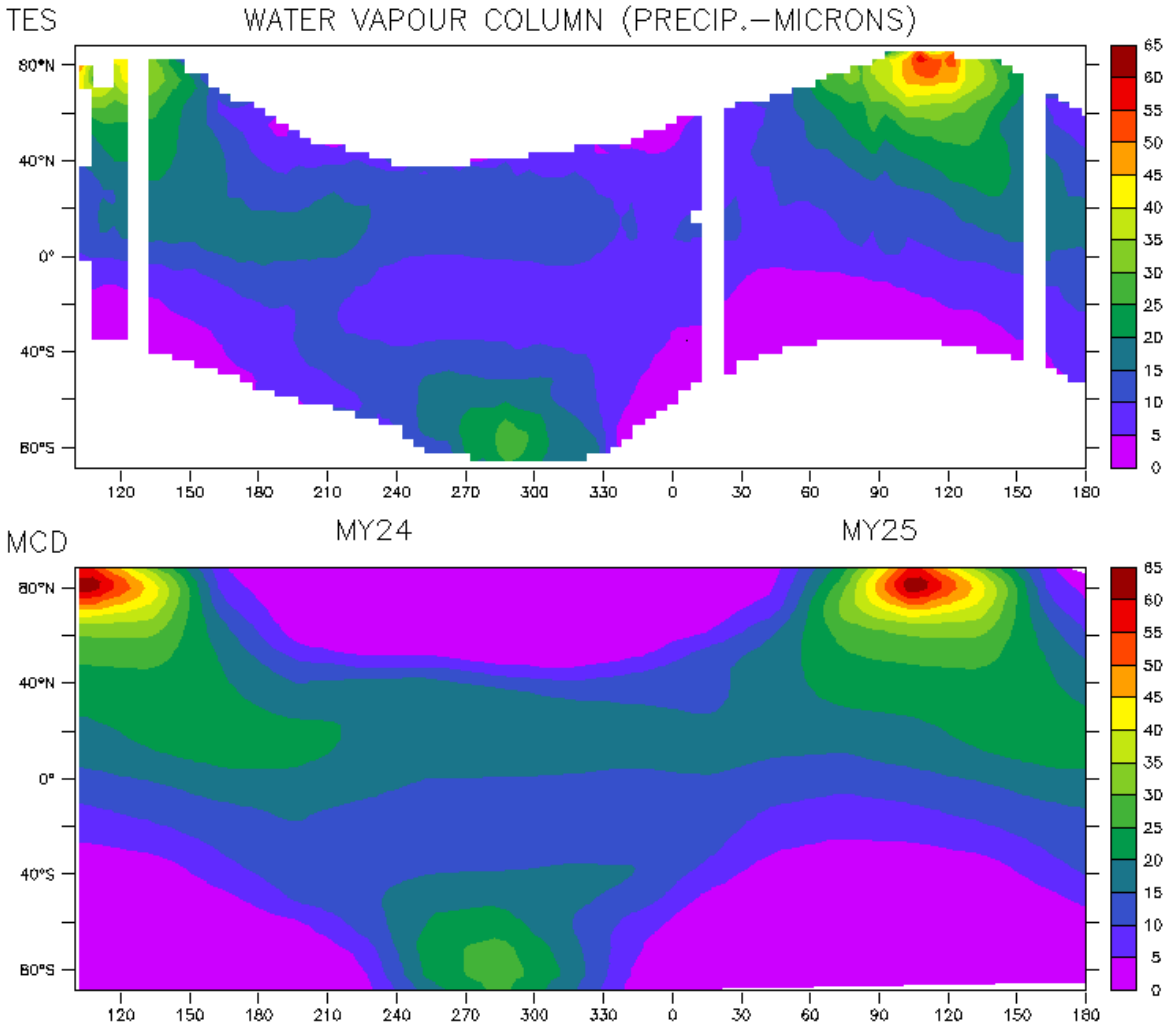

Figure 7.1 : Zonal values of water vapour column (in precipitable microns), over Mars Year 24-25 (from Ls=102 in MY24 up to Ls=180 in MY25, i.e. prior to the global dust storm). Top: TES measurements. Bottom: MCD data.

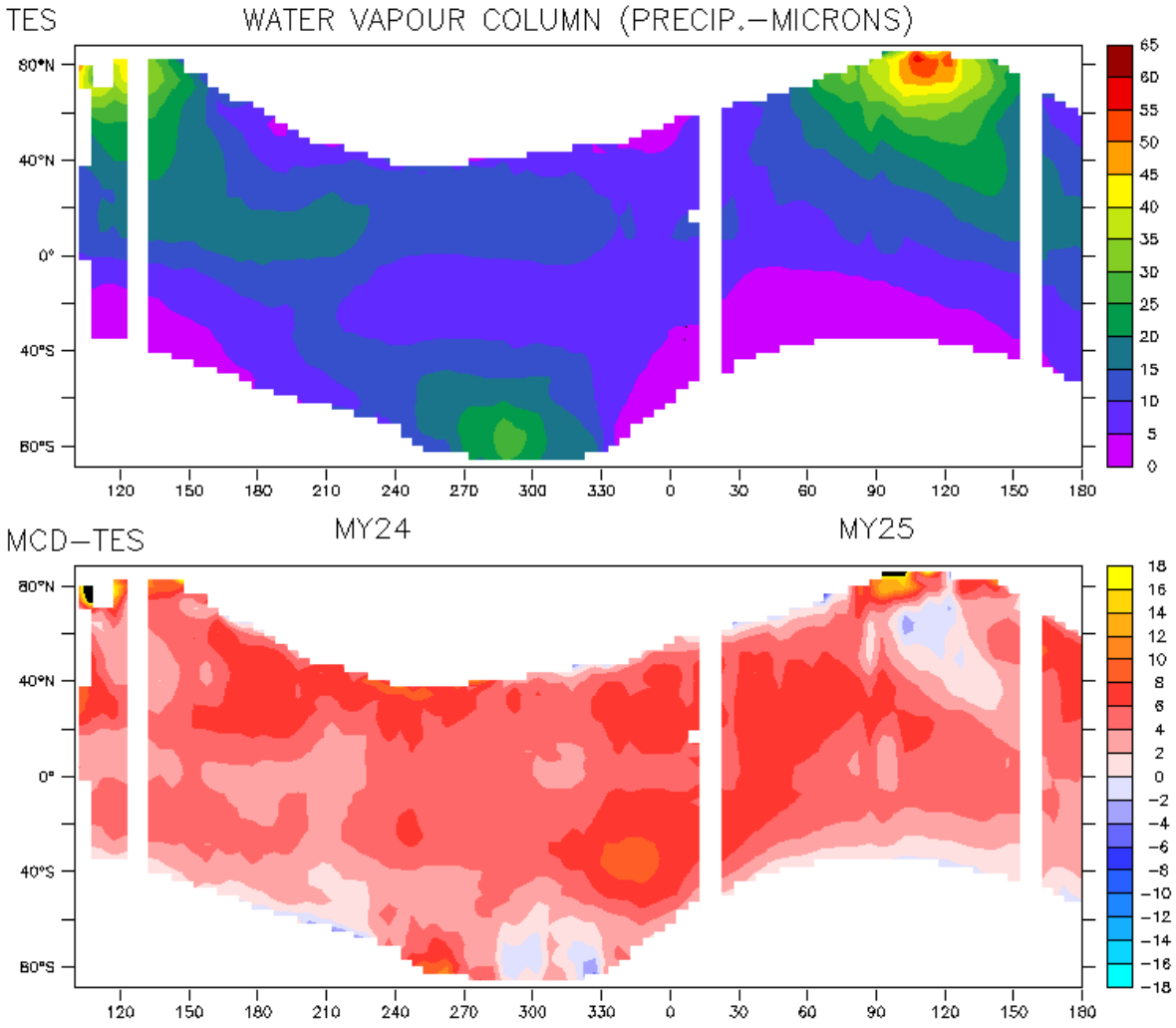

Figure 7.2 : Top: Zonal values of water vapour column (in precipitable microns), over Mars Year 24-25 (from Ls=102 in MY24 up to Ls=180 in MY25, i.e. prior to the global dust storm) measured by TES.
Bottom: Difference between MCD and TES zonal values of water vapour column. Black regions correspond to off-scale values.

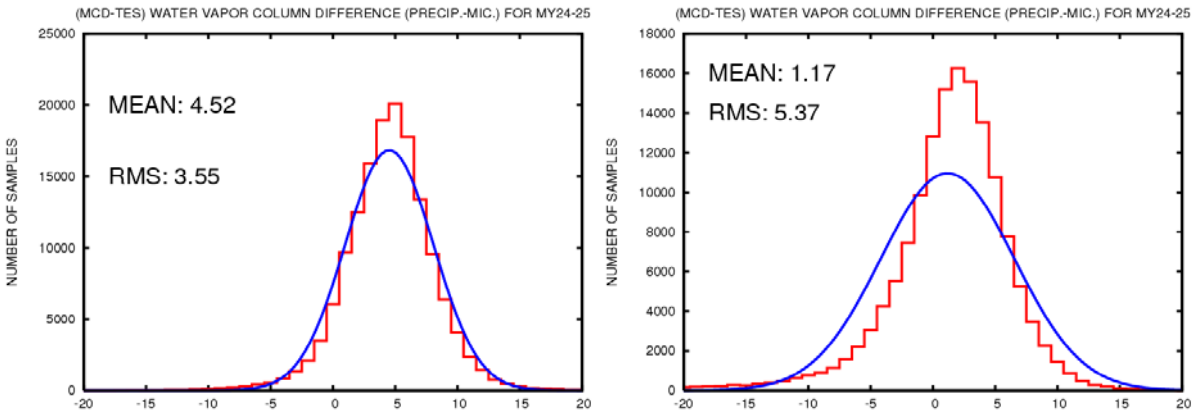

Figure 7.3 : Distribution of zonal water vapour column differences, between MCD and TES data. Statistics were computed over Mars Years 24 and 25 (from Ls=102.5 in MY24 until Ls=180 in MY25), using bins of 1 precipitable microns. Given mean and RMS values are computed for the histograms; the blue curves are normal distributions of same mean and RMS. Left plot is for latest TES dataset and right plot is for an earlier release of the TES data which was used to calibrate the GCM runs from which the MCD is derived..

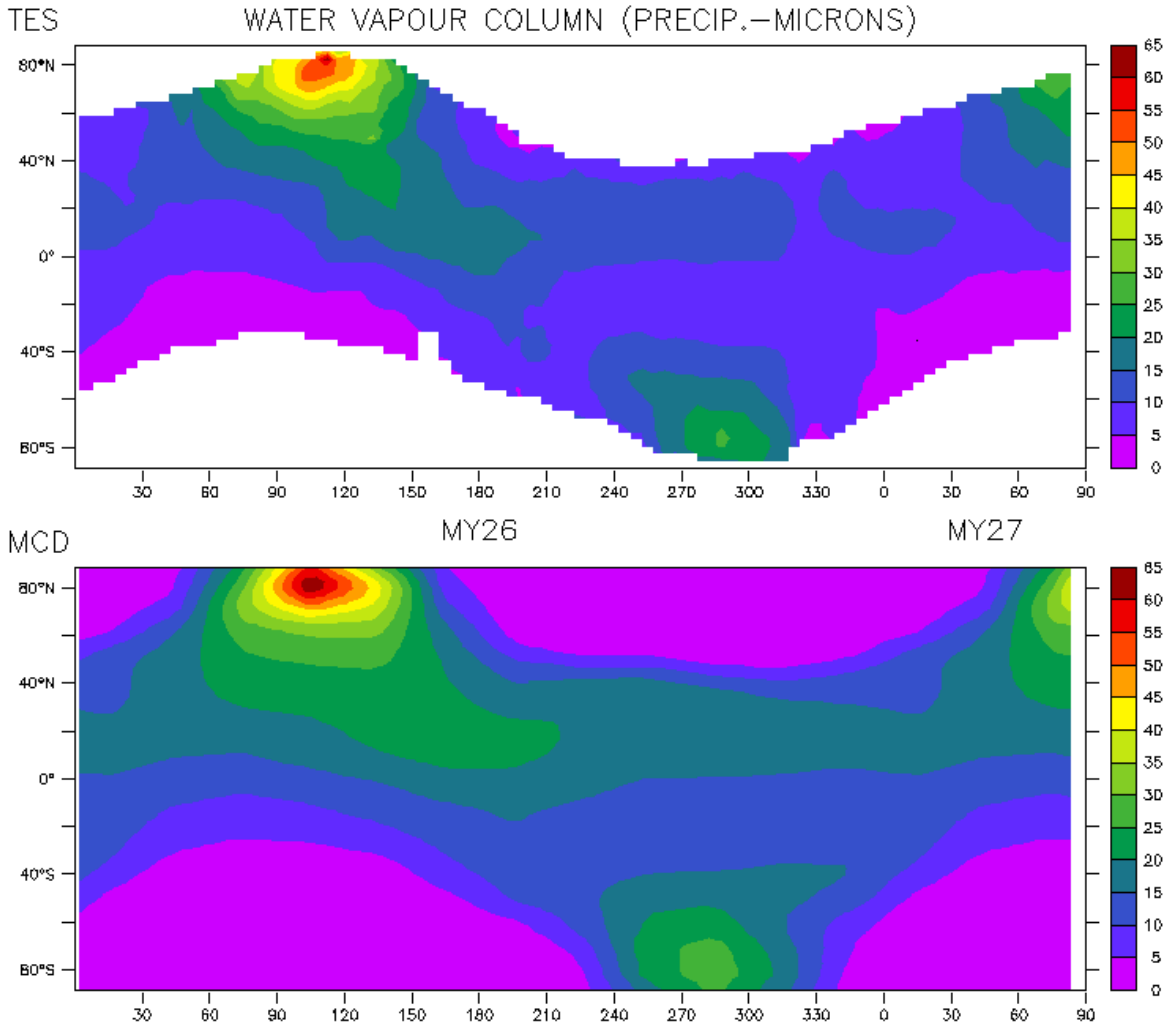

Figure 7.4 : Zonal values of water vapour column (in precipitable microns), over Mars Year 26-27 (from Ls=0 in MY26 up to Ls=85 in MY27). Top: TES measurements. Bottom: MCD data.

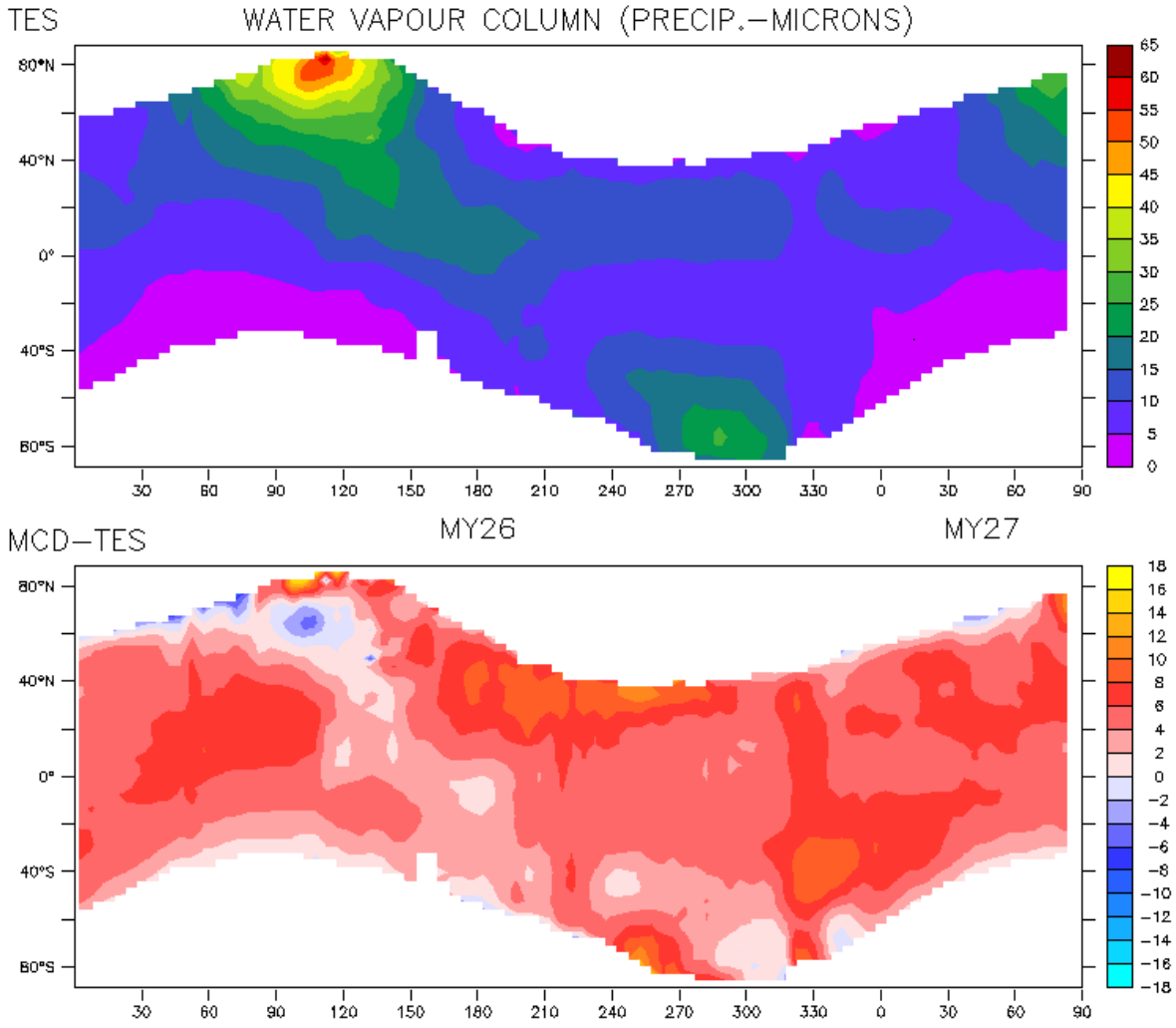

Figure 7.5 : Top: Zonal values of water vapour column (in precipitable microns), over Mars Year 26-27 (from Ls=0 in MY26 up to Ls=85 in MY27) measured by TES.
Bottom: Difference between MCD and TES zonal values of water vapour column.

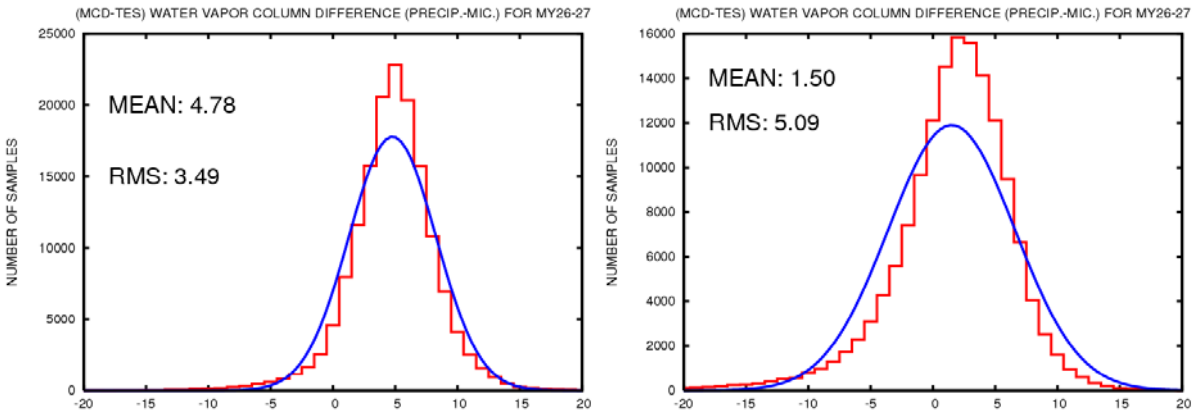

Figure 7.6 : Distribution of zonal water vapour column differences, between MCD and TES data. Statistics were computed over Mars Years 26 and 27 (from Ls=0 in MY26 up to Ls=85 in MY27), using bins of 1 precipitable microns. Given mean and RMS values are computed for the histograms; the blue curves are normal distributions of same mean and RMS. Left plot is for latest TES dataset and right plot is for an earlier release of the TES data which was used to calibrate the GCM runs from which the MCD is derived..